YAŞAR UNIVERSITY
GRADUATE SCHOOL OF NATURAL AND APPLIED SCIENCES
MASTER THESIS

WIDE-AREA DAMPING OF POWER SYSTEM OSCILLATIONS USING MODEL PREDICTIVE CONTROL

Munir Aminu HUSEIN

Thesis Advisor: Assist. Prof. Emrah BIYIK

Department of Electrical and Electronic Engineering

İZMİR, TURKEY
2014

I certify that I have read this thesis and that in my opinion it is fully adequate, in scope and in quality, as a dissertation for the degree of master of science.

_____

Assist. Prof. Dr. Emrah BIYIK (Supervisor)

I certify that I have read this thesis and that in my opinion it is fully adequate, in scope and in quality, as a dissertation for the degree of master of science.

_____

Assist. Prof. Dr. Hacer SEKERCI

I certify that I have read this thesis and that in my opinion it is fully adequate, in scope and in quality, as a dissertation for the degree of master of science.

_____

Assist. Prof. Dr. Erginer UNGAN

_____

Prof. Dr. Behzat GÜRKAN
Director of the Graduate School

ABSTRACT

Electromechanical oscillations in power systems have been observed ever since synchronous generators were interconnected to provide reliability and higher generation capacity, and have become a severe threat for the safe and economic operation of modern interconnected power grids. With the development of wide-area measurement system (WAMS) and deployment of synchronized Phasor Measurement Units (PMU), Wide-Area Damping Controller (WADC) is designed to enhance the damping of these oscillations.

This thesis develops a systematic procedure of designing Wide-Area Damping Controller (WADC) using Model Predictive Control (MPC) technique to damp electromechanical oscillations in power system. The proposed technique is based on a linearized discrete-time state space model of a power system. The MPC controller computes the optimal input sequence over a chosen time horizon by solving a quadratic programming problem and sends these signals to the excitation system of a remote generator where it will supplement the local damping controllers. Power System Stabilizers were used as local damping controllers in this thesis.

The effectiveness and robustness of the proposed Model Predictive Controller for wide-area damping control scheme have been verified by two study systems. The first test system is the IEEE 4-Generator 2-Area test system. The second one is the IEEE 16-Generator 5-Area test system.

Simulation results of these test systems reveal that the proposed MPC wide-area damping controller damps the inter-area oscillations effectively under varying operation conditions and different disturbances.

Keywords: Power System, Model Predictive Control, Inter-area Oscillations, Wide-area Damping, Phasor Measurement Unit

ÖZET

Güç sistemlerinde güvenli ve yüksek kapasitede güç üretimi sağlayan senkron jeneratörler elektromekanik salınımlara sebep olmaktadırlar. Bu salınımlar kimi durumlarda modern elektrik şebekelerinin güvenli ve ekonomik işletilmesini tehdit eder boyuta gelmektedirler. Geniş Alan Ölçüm Üniteleri (WAMS) ve Senkronize Faz Ölçüm Uniteleri'nin (PMU) yaygınlaşması ile birlikte bu salınımları sönümlemek için Geniş Alan Baskılama Denetleyicilerinin (WADC) tasarımları mümkün olmaya başlamıştır.

Bu tezde, güç sistemlerinde alanlar arası salınımları sönümlemek için Model Öngörümlü Denetleç (MPC) yöntemini kullanan bir Geniş-Alan Baskılama Denetleyicisi tasarlanmıştır. Önerilen yöntem, güç sistemlerinin lineer kesikli zamanlı durum uzayı modelini temel almaktadır. MPC denetleyici belirli bir tahmin ufku içerisinde en iyi kontrol sinyalini Karesel Programlama problemini çözerek hesaplamakta ve sonrasında bu sinyalleri uzaktaki jeneratörlerde bulunan yerel salınımları sönümleyici denetleyicilere ek kontrol sinyali olarak göndermektedir. Bu tezde yerel salınımları sönümlemek için Güç Sistemi Kararlı Kılıcısı (PSS) kullanılmaktadır.

Tasarlanan MPC denetleyici önce ideal durumda test edilmiş (bütün durum değişkenleri gözlenebilir ve kontrol edilebilir, haberleşme ve hesaplama gecikmeleri ihmal edilebilir Kabul edilerek), sonrasında, önerilen metodun durum değişkeni tahmin hataları ve hesaplama ve haberleşme gecikmelerinin olduğu durumlardaki etkinliği değerlendirilmiştir.

Önerilen denetleyicinin etkinliği ve gürbüzlüğü iki ayrı test sistemi üzerinde teyit edilmiştir. Ele alınan ilk system IEEE 4-jeneratör, 2-Alan test sistemi, ikincisi ise IEEE 16 Jeneratör, 68 Baralı test sistemidir. Bu test sistemleri üzerinde yapılan benzetim çalışmaları sonucunda MPC denetleyicinin değişken çalışma koşullarında ve farklı bozucu etkilere karşı geniş alan salınımlarını başarıyla sönümlediği, ve ayrıca geniş-alan sinyallerindeki gecikmelere karşı gürbüz olduğu gözlemlenmiştir.

Anahtar kelimeler: Güç sistemleri, Model öngörümlü denetleç, Alanlar-arası salınımlar, Geniş-alan sönümleme

ACKNOWLEDGEMENTS

I would like to express my deepest gratitude to my research advisor, Assist. Prof. Dr. Emrah Biyik, for his patience, support and guidance throughout my MSc research. It has been a privilege for me to work under his supervision and I am his student forever.

I thank the members of my thesis committee, Assist. Prof. Dr. Hacer SEKERCI and Assist. Prof. Dr. Erginer UNGAN, for devoting their time to read this manuscript and providing useful feedback.

I also wish to extend my sincerest appreciation to the entire staff of Electrical and Electronic Engineering of Yasar University, for their support throughout my studies. Many thanks to Prof. Mustafa Gunduzalp and Assoc. Prof. Mustafa Secmen for their invaluable guidance.

I acknowledged the help and support I received from Smart Grid Lab of Kookmin University, South Korea. Special thanks go to Prof. Il Yop Chung, his enthusiasm is a strong source of inspiration.

I thank my brother and classmate, Habibu Aminu Husein, and the rest of my family and friends, who have sustained and supported me in my endeavors for so many years. I feel so lucky to have been blessed with them.

Munir HUSEIN
İzmir, 2014

TEXT OF OATH

I hereby declare that this thesis is my own work and that, to the best of my knowledge and belief, it reproduces no material previously published or written or material which has been accepted for the award of any other degree or diploma, except where due acknowledgement has been made in the text.

_____ (Signed)

Munir Aminu Husein (Name of student)

TABLE OF CONTENT

TABLE OF CONTENT (CONT.)

TABLE OF CONTENT (CONT.)

INDEX OF FIGURES

INDEX OF ABBREVIATIONS

MIMO	Multi-Input Multi-Output
MPC	Model Predictive Control
SCADA	Supervisory Control And Data Acquisition
EMS	Energy Management System
WAMS	Wide Area Measurement System
PMU	Phasor Measurement Unit
GPS	Global Positioning System
WADC	Wide Area Damping Controller
SISO	Single-Input Single-Output
PSS	Power System Stabilizer
FACTS	Flexible AC Transmission Systems
LMI	Linear Matrix Inequality
WACS	Wide Area Control System
WECC	Western Electric Coordinating Council
LPSS	Local Power System Stabilizer

INDEX OF SYMBOLS

Symbols	Explanations
A	State matrix of state-space model
B	Input-to-state matrix of state-space model
C	State-to-output matrix of state-space model
Δt	Sampling time
k	MPC control time step
J	Cost function for optimization
N_C	Control horizon
N_P	Prediction horizon
$W_{\Delta u}$	Weighting factor for control increments
W_u	Weight on manipulated variable
W_y	Weighting factor for predicted error
ω	Generator speed
δ	Generator rotor angle
E_{fld}	Generator field voltage
$E_d^{'}, E_q^{'}$	Direct and quadrature axis components of stator voltage
$X_d, X_d^{'}, X_d^{''}$	Direct axis synchronous, transient and subtransient reactances
$X_q, X_q^{'}, X_q^{''}$	Quadrature axis synchronous, transient and subtransient reactances
$\psi_d^{''}$ $\psi_q^{''}$	Direct and quadrature axis air gap flux linkage
ψ_{1d}, ψ_{1q}	Direct and quadrature axis amortisseur circuit flux linkage
$x, \hat{x}$	Power system states and estimated states
$y, \hat{y}$	Measured and estimated output
V_{ref}	Exciter reference voltage
y_{ref}	Output reference
ω_{ref}	Generator speed reference

CHAPTER 1

INTRODUCTION

1.1 Background and Motivation

Electric power systems are among the largest structural achievements of man. Electro-mechanical oscillations between interconnected synchronous generators are phenomena inherent in these systems [1]. The stability of these oscillations is of immense importance, and is a prerequisite for stable and secure system operation. If not damped out quickly, these oscillations may lead to generator outages, line tripping, network splitting and even blackouts [2]. In terms of oscillation ranges and frequencies, electromechanical oscillations can be divided into two categories, local mode oscillations and inter-area mode oscillations.

Local mode oscillations, also called plant mode, occur when a generator (or group of generators) at a station is swinging against the rest of the system. These oscillations have frequencies in the range 0.7 to 2.0 Hz [3]. The characteristics of these oscillations were understood, they were studied adequately, and satisfactory solutions to their stability problems were well developed.

Inter-area modes are associated with the swinging of many generators in one part of the system against generators in other parts. Their frequencies are in the range 0.1 to 0.7 Hz [3]. The characteristics of these modes of oscillations, and the factors influencing them, are far more complex to study, and to control. A detail representation of the entire interconnected system is required to study inter-area mode [4]. This thesis deals with inter-area oscillations.

Heavy power transfer across weak tie-lines or high-gain exciters are the main cause of Inter-area oscillations [3]. Large power systems typically exhibit multiple dominant inter-area swing modes, which are associated with the dynamics of power transfers and involve groups of machines oscillating relative to each other. When present in a power

system, these oscillations limit the amount of power transfer on the regions containing the groups of coherent generators [4].

In recent times, many instances of unstable oscillations, involving inter-area modes in large power systems have been observed, both in studies and in practice: at 0.6 Hz in the Hydro-Quebec system [5], at 0.2Hz in the western North-American interconnection [6], at 0.15-0.25 Hz in Brazil [7] and at 0.19-0.36 Hz in the UCTE/CENTREL interconnection in Europe [8]. The recent 2003 blackout in eastern Canada and US was accompanied by severe 0.4 Hz oscillations in several post-contingency stages [9]. In China, within the year 2008, two system-wide low-frequency oscillations incidences occur respectively in the South China and Central China grids [10].

Many other incidents of system outage resulting from these oscillations have been reported over the years, and as such, they are increasingly becoming a cause of concern. This has led to a renewed effort in understand the nature of these oscillations, methods for systematically studying them, and control techniques by which they can be stabilized.

The traditional control approach in use today to damp these oscillations is to employ conventional Local Power System Stabilizers (LPSS) that provide supplementary control action through the generator excitation systems. In recent times, Supplementary Modulation Controllers (SMC) are added to Flexible AC Transmission Systems (FACTS) devices to damp inter-area oscillations. These controllers are effective in damping local modes, and if carefully tuned [11] may also damp inter-area modes up to a certain transmission loading. Their effectiveness in damping inter-area mode is limited because these controllers are single-input single-output non-coordinated controllers that usually use local inputs and cannot always be effective in solving the problem due to two main shortcomings.

First, these local controllers are designed to have fixed parameters derived from linearized model around a certain nominal operating point. Therefore conventional local

controllers designed by classical control techniques have their validity restricted to a neighborhood of this point. But power systems constantly experience changes in operating conditions due to variations in generation and load patterns. Furthermore, some uncertainty is inevitably introduced into a power system model due to inaccurate approximation of the power system parameters, neglected high frequency dynamics and invalid assumptions made in the modeling process.

Second, it has been proven that under certain operating conditions, an inter-area mode may be controllable from one area and be observable from another [12]. In such cases, local controllers lack global observation of inter-area modes and hence are not effective for the damping of that mode.

The recently developed Wide-Area Control System (WACS) technologies offer a great potential to overcome the shortcomings of conventional local controllers in damping inter-area oscillations. With the fast development of global positioning system (GPS) based Phasor Measurement Units (PMU), dynamic data of power systems, such as voltage, current, angle, and frequency are reliable available and can be accurately measured, synchronized and transferred in the range of the whole power system by Wide-Area Measurement Systems (WAMS) [13, 14].

This advancement makes possible the construction of wide-area damping control systems. In contrast to conventional local controls, wide-area damping controls have many benefits. Reference [15] shows that wide-area damping controls are more efficient than local controls in preventing loss of synchronism and local controls need large gain (from 4 to 20 times more) than wide-area damping controls [16] to achieve a similar damping effect.

1.2 Literature Review on Wide Area Damping Control for Power System

Wide-area control refers to any control that requires some communication link to either gather the input or to send out control signals [17]. Although control using signals obtained remotely requires additional communication equipments, it is likely that the

cost of such equipment would be offset by additional operating flexibility gained by the control.

Many researchers achieved good results by applying wide area measurement to the design of wide-area control system for power system oscillation damping. One promising approach is to design wide-area measurement based controllers that provide control actions through generator excitation systems supplemental to the action of local PSS.

Wide-area damping controllers were perhaps first designed by Magdy et. al. [12]. They found that if wide-area signals are applied to the local controllers, the system dynamic performance can be enhanced with respect to inter-area oscillations.

Kamwa, Grondin and Hebert [18] propose a decentralized/hierarchical structure for a wide-area control system. Wide-area signals based PSS is used to provide additional damping to local ones. A sequential optimization procedure is used to tune the global and local loop of the proposed controller.

In [19], a systematic procedure of designing a wide-area controller is presented. The synthesis of the controller is defined as a problem of mixed H_2/ H_∞ output-feedback control with regional pole placement and is resolved by the linear matrix inequality (LMI) approach.

Reference [20] uses multi-agent concepts to coordinate several supervisory PSSs (SPSS) based on remote signals and exchanging information with local PSSs to improve power systems stability. The SPPs is designed by H_∞ optimization methods. Rule based fuzzy-logic and robust control techniques are used to deal with uncertainties introduced by nonlinear terms and operating conditions.

Defining the differences between post-fault transmission power and its steady state value as a cost function, paper [21] optimizes TCSC parameters based on sensitivity analysis to provide the maximum damping for various operation conditions. Paper [22] introduces angular speeds of remote generators to a PSS to improve its damping to inter-area oscillations.

As can be seen from the above works, various control techniques were used in designing these controllers. In recent years, Model Predictive Control (MPC) was found to be an attractive control algorithm for designing wide-area damping controllers. At a control instant, the MPC algorithm computes an open-loop sequence of inputs in order to optimize future plant behavior. The first input in the optimal sequence is injected into the plant, and the entire optimization is repeated at subsequent control steps [23].

This powerful control technique will be employed in this thesis to design wide-area damping controller to damp out inter-area oscillations in power systems.

1.3 Thesis Organization

The thesis is organized in five chapters. A brief summary of the chapters are as follows:

Chapter 1 starts with the background and motivation of the thesis. A literature review that summarizes the research in wide-area damping control is presented. Finally, the organization of the thesis is presented.

Chapter 2 introduces Model Predictive Control, its strategy, algorithms, and applications. Its advantages and disadvantages are outline. Finally, review of MPC applications in power system is discussed.

Chapter 3 presents the procedure for designing wide-area MPC controller to damp inter-area oscillations in power system. A complete power system, including synchronous generator, excitation system, governor and power system stabilizer are then modeled. The proposed MPC scheme is outline, with detail state space representation, prediction formulation, and cost function optimization.

Chapter 4 provides two case studies to illustrate the effectiveness of wide-area MPC controller in damping power system oscillations. The first case study uses IEEE 4-Generator 2-area Test System, and the second uses IEEE 16-Generator 5-Area Test System.

Chapter 5 concludes the work, summarizing the findings as well as contribution related to the procedures in this thesis. Furthermore, possible future research topics were suggested.

Additionally, this thesis includes three appendices. Appendix A and B provide the dynamic data of IEEE 4-Generator 2-area Test System and IEEE 16-Generator 5-Area Test System respectively. Appendix C is a brief introduction of Power System Toolbox (PST).

CHAPTER 2

OVERVIEW OF MODEL PREDICTIVE CONTROL

2.1 What is Model Predictive Control?

Model Predictive Control (MPC), also referred to as 'Receding Horizon Control' and 'Moving Horizon Optimal Control', is a form of control in which a performance index is optimized with respect to some future control sequence, using predictions of the output signal based on the system model, while satisfying constraints on inputs and output/states.

The name 'Model Predictive Control' is from an idea of employing an explicit model of the plant to be controlled which is used to predict the future output behavior.

2.2 Model Predictive Control Strategy

Model Predictive Control, MPC, usually contains the following three ideas [24]:

(i) Explicit use of a model to predict the system output along a future time horizon

(ii) Calculation of a control sequence to optimize a performance index

(iii) A receding horizon strategy, so that at each instant the horizon is moved towards the future, which involves the application of the first control signal of the sequence calculated at each step

The methodology of all the controllers belonging to the MPC family is characterized by the following strategy illustrated as shown in Fig. 2.1.

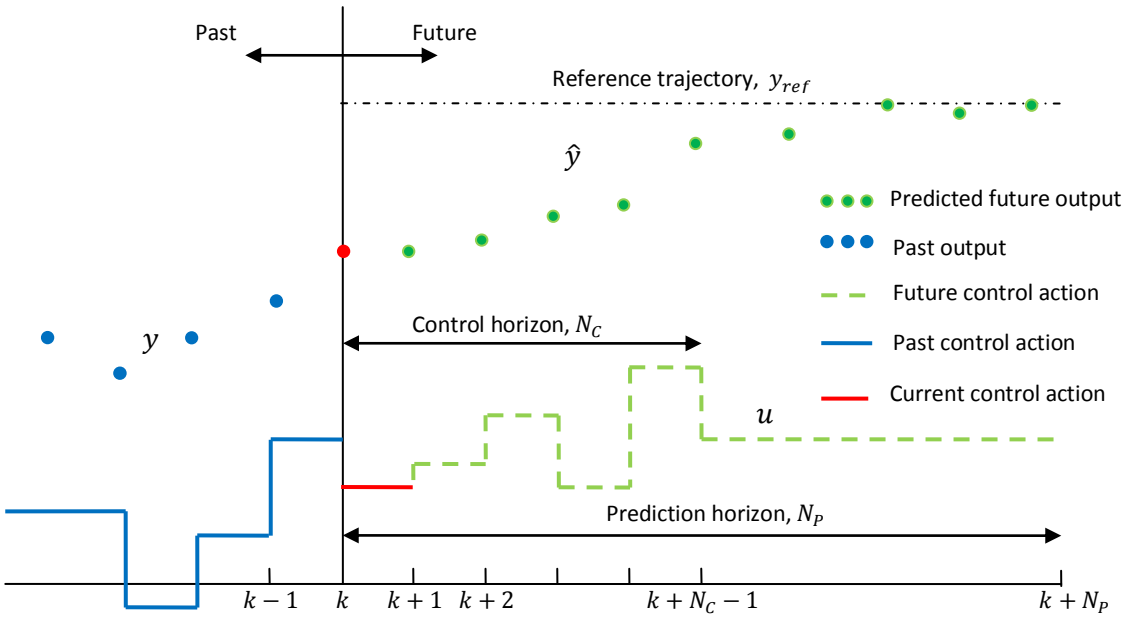

Fig. 2.1 Basic Model Predictive Control Strategy

The strategy is described as follows:

- At each instant k, the model is used to predict the future outputs, $\hat{y}(k+i|k), \text{for } i = 1 \ldots N_P$, were N_P (a finite integer ≥ 1) is called the prediction horizon. These depend upon the known values up to instance k (past inputs and outputs), including the current output (initial condition) $y(k)$ and on the future control signals $u(k+i|k), i = 0 \ldots N_P - 1$, to be calculated. (Note – the notation $x(k+i|k)$ indicates the value of x at time instant $k+i$ calculated at instant k).

- At the current sampling instant, k, the MPC strategy computes a set of N_C control moves $u(k), u(k+1) \ldots u(k+N_C-1)$. The number of these control moves, $N_{C,}$ is called control horizon. These moves were held constant after N_C. The objective of the MPC control computations is to determine a sequence of control moves so that the predicted outputs, $\hat{y}(k+i), i = 1, 2, \ldots, N_P$, reaches the set point y_{ref}, in an optimal manner. These control moves are obtained by

optimizing an objective function. The objective function usually takes the form of a quadratic function of the errors between the predicted output signal and the predicted reference trajectory. If the criterion is quadratic, the model is linear, and there are no constraints, an explicit solution can be obtained; otherwise an iterative optimization method has to be employed.

- Only the current control signal $u(k|k)$ is transmitted to the plant. At the next sampling instant $y(k+1)$ is measured and step 1 is repeated and all sequences brought up to date. Thus $u(k+1|k+1)$ is then calculated using the receding horizon approach. The receding horizon concept is a distinguishing feature of the MPC. Although a sequence of N_C control moves is calculated at each sampling instant, only the first move is actually implemented while ignoring the rest of the sequence. Then a new sequence is computed at the next sampling instant, after new measurements become available; again only the first input move is implemented. This process is repeated at each sampling instant.

2.3 Components of Model Predictive Control

Three components are common to all Model Predictive Controllers [24], and there are several options of representing each components resulting in different MPC algorithms. These components are:

- Prediction Model
- Objective Function
- Obtaining the Control Law

In order to explain the function of each component, a basic MPC structure is shown in Fig. 2.2.

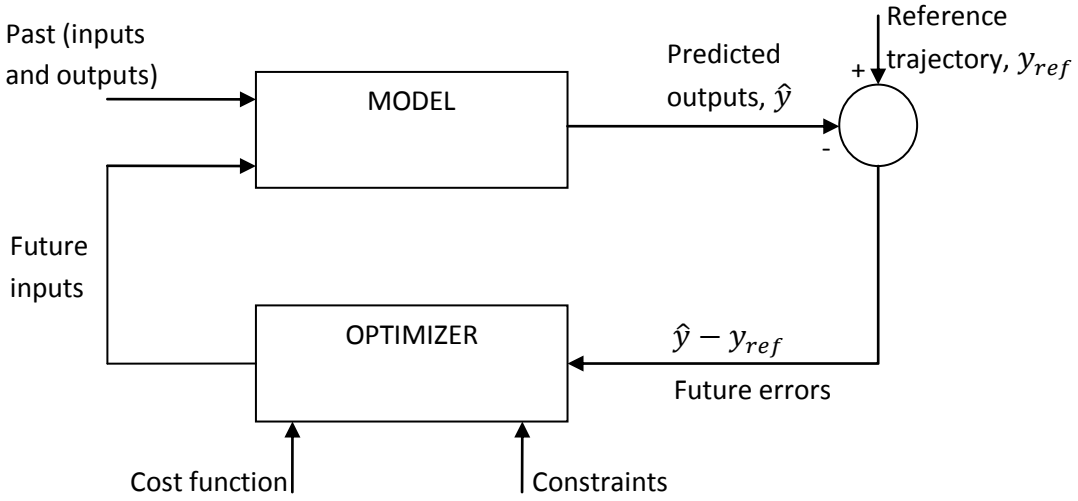

Fig. 2.2 Basic Structure of MPC (Modified from [24])

2.2.1 Prediction Model

The model is the cornerstone of MPC; model selection is the most important part of MPC design [25]. A model of the system is used to predict the future plant outputs, based on past and current values and on the proposed optimal future control actions. These actions are calculated by the optimizer taking into account the cost function as well as the constraints.

The model must be able to capture the system's dynamics to accurately predict the future outputs and at the same time be intuitive and simple to implement and analyzed.

2.2.1 Objective Function

The optimizer is another crucial part of the MPC strategy as it provides the control actions. Various MPC algorithms use different cost function for obtaining the control law. Selection of the cost function is an area of both engineering and theoretical judgment. The main aim is for the future output (*y)* on the considered horizon follow a determined reference trajectory(y_{ref}) and at the same time the control effort (Δu) necessary for doing so should be penalized.

2.2.3 *Obtaining the Control Law*

To obtain the values of $u(t+k\,|t)$ it is necessary to minimize an objective function, J. To obtain this the value of predicted outputs $\hat{y}(t+k\,|t)$ are calculated as a function of past values of inputs and outputs and future control signals, making use of the model chosen and substituted in the cost function, obtaining an expression whose minimization leads to the looked-for values. An analytical solution can be obtained for the quadratic criterion if the model is linear and there are no constraints, otherwise an iterative method of optimization should be used.

2.4 Mathematical Formulation of MPC

There are many different types of models used in MPC formulation, the choice depend on which algorithm is employed. Recent years have seen the growing popularity of predictive control design using state-space design methods [26], therefore a linearized, discrete-time, state-space model will be used in this section to derive MPC prediction equations, objective functions and constraints.

Consider the linearized, discrete-time, state-space model of the plant, in the form:

$$\begin{aligned} x[k+1\,|\,k] &= Ax[k\,|\,k] + Bu[k|k] \\ y[k|k] &= C_y x[k|k] \\ z[k|k] &= C_z x[k|k] \end{aligned} \tag{2.1}$$

where x is a d_x-dimensional state vector, u is a d_u-dimensional input vector, y is a d_y-dimensional measured output vector, and z is a d_z-dimensional vector of output which are to be controlled, either to particular set-points, or to satisfy some constraints, or both. The index k counts 'time steps'. The variables in y and z usually overlap, and frequently are the same; meaning all the controlled outputs will frequently be measured. Often, it will be assumed that$y \equiv z$, and C will be used to denote both C_y and C_z.The index k counts 'time steps'. Equation 2.1 can then be simplified to:

$$x[k+1|k] = Ax[k|k] + Bu[k|k] \quad (2.2)$$

$$y[k|k] = Cx[k|k] \quad (2.3)$$

In practice, it should not be assumed that all states variables can be measured directly and exactly, so an estimated $\hat{x}[k|k]$ will be used to replace the real state, $x[k|k]$. Correspondingly, $\hat{x}[k+1|k]$ and $\hat{y}[k+1|k]$ denote the predictions of variables *x* and *y* at time $k + 1$, on the assumption that one input $\hat{u}[k|k]$ is applied at time *k*. So, Equation (2.2) and (2.3) can be further changed to:

$$\hat{x}[k+1|k] = A\hat{x}[k|k] + B\hat{u}[k|k] \quad (2.4)$$

$$\hat{y}[k|k] = C\hat{x}[k|k] \quad (2.5)$$

The predictions can now be made of a future states over a given prediction horizon, N_P, by iterating Equation (2.4) and (2.5)

$$\hat{x}[k+1|k] = A\hat{x}[k|k] + B\hat{u}[k|k]$$

$$\hat{x}[k+2|k] = A\hat{x}[k+1|k] + B\hat{u}[k+1|k]$$

$$\hat{x}[k+2|k] = A\hat{x}[k+1|k] + B\hat{u}[k+1|k]$$

$$A^2\hat{x}[k|k] + AB\hat{u}[k|k] + B\hat{u}[k+1|k] \quad (2.6)$$

.

.

.

$$\hat{x}[k+N_P|k] = A\hat{x}[k+N_P-1|k] + B\hat{u}[k+N_P-1|k]$$

$$A^{N_P}\hat{x}[k|k] + A^{N_P-1}B\hat{u}[k|k] + \cdots + B\hat{u}[k+N_P-1|k]$$

The above equations can be expressed in the matrix-vector form:

$$\begin{bmatrix} \hat{x}[k+1|k] \\ \hat{x}[k+2|k \\ \vdots \\ \hat{x}[k+N_P|k] \end{bmatrix} = \begin{bmatrix} A \\ A^2 \\ \vdots \\ A^{N_P} \end{bmatrix} \hat{x}[k|k] + \begin{bmatrix} B & 0 & 0 \\ AB & B & 0 \\ \vdots & \vdots & \vdots \\ A^{N_P-1}B & A^{N_P-2}B & B \end{bmatrix} \times \begin{bmatrix} \hat{u}[k|k] \\ \hat{u}[k+1|k] \\ \vdots \\ \hat{u}[k+N_P-1|k] \end{bmatrix} \quad (2.7)$$

The input vector $\hat{u}[k+i|k]$ changes only at the first T_C steps, namely at the times $k, k+1, \ldots, k+N_C-1$, and will remain constant thereafter. That is to say, $\hat{u}[k+i|k] = \hat{u}[k+N_C-1]$ for $N_C \leq i \leq N_P-1$. The items in the input matrix corresponding to the same $\hat{u}[k+i|k]$ in Equation (2.7) to obtain:

$$\begin{bmatrix} \hat{x}[k+1|k] \\ \hat{x}[k+2|k] \\ \vdots \\ \hat{x}[k+H|k] \\ \vdots \\ \hat{x}[k+N_P|k] \end{bmatrix} = \begin{bmatrix} A \\ A^2 \\ \vdots \\ A^{N_C} \\ \vdots \\ A^{N_P} \end{bmatrix} \hat{x}[k|k] +$$

$$\begin{bmatrix} B & 0 & \cdots & 0 \\ AB & B & \cdots & 0 \\ \vdots & \vdots & \cdots & \vdots \\ A^{N_C-1}B & A^{N_C-2} & \cdots & B \\ \vdots & \vdots & \cdots & \vdots \\ A^{N_P-1}B & A^{N_P-2}B & \cdots & \sum_{i=0}^{N_P-N_C} A^i B \end{bmatrix} \begin{bmatrix} \hat{u}[k|k] \\ \hat{u}[k+1|k] \\ \vdots \\ \hat{u}[k+N_P-1|k] \end{bmatrix} \quad (2.8)$$

In the predictive control, the input change $\Delta\hat{u}[k+i|k]$ is often computed rather than $\hat{u}[k+i|k]$. Defining that $\Delta\hat{u}[k+i|k] = \hat{u}[k+i|k] - \hat{u}[k+i-1|k]$:

$$\begin{bmatrix} \hat{u}[k|k] \\ \hat{u}[k+1|k] \\ \vdots \\ \hat{u}[k+N_P-1|k] \end{bmatrix} = \begin{bmatrix} I \\ I \\ \vdots \\ I \end{bmatrix} u[k-1] + \begin{bmatrix} I & 0 & \cdots & 0 \\ I & I & \vdots & 0 \\ \vdots & \vdots & \vdots & \vdots \\ I & I & \cdots & I \end{bmatrix} \times \begin{bmatrix} \Delta\hat{u}[k|k] \\ \Delta\hat{u}[k+1|k] \\ \vdots \\ \Delta\hat{u}[k+N_P-1|k] \end{bmatrix} \quad (2.9)$$

$u[k-1]$ is now known. Subtituting Equation (2.9) into Equation (2.8) results in:

$$\begin{bmatrix} \hat{x}[k+1|k] \\ \hat{x}[k+2|k] \\ \vdots \\ \hat{x}[k+N_C|k] \\ \hat{x}[k+N_C+1|k] \\ \vdots \\ \hat{x}[k+N_P|k] \end{bmatrix} = \begin{bmatrix} A \\ A^2 \\ \vdots \\ A^{N_C} \\ A^{N_C+1} \\ \vdots \\ A^{N_P} \end{bmatrix} \hat{x}[k|k] + \begin{bmatrix} B \\ AB+B \\ \vdots \\ \sum_{i=0}^{N_C-1} A^i B \\ \vdots \\ \sum_{i=0}^{N_P-1} A^i B \end{bmatrix} u[k-1]$$

$$+ \begin{bmatrix} B & 0 & \cdots & 0 \\ AB+B & B & \cdots & 0 \\ \vdots & \vdots & \cdots & \vdots \\ \sum_{i=0}^{N_C-1} A^i B & \sum_{i=0}^{N_C-1} A^i B & \cdots & B \\ \vdots & \vdots & \cdots & \vdots \\ \sum_{i=0}^{N_P-1} A^i B & \sum_{i=0}^{N_P-1} A^i B & \cdots & \sum_{i=0}^{N_P-1} A^i B \end{bmatrix} \begin{bmatrix} \Delta\hat{u}[k|k] \\ \Delta\hat{u}[k+1|k] \\ \vdots \\ \Delta\hat{u}[k+N_C-1|k] \end{bmatrix} \tag{2.10}$$

Finally, the predictions of y over the whole prediction horizon are given by:

$$\begin{bmatrix} \hat{y}[k+1|k] \\ \hat{y}[k+2|k \\ \vdots \\ \hat{y}[k+N_P|k] \end{bmatrix} = \begin{bmatrix} C & 0 & \cdots & 0 \\ 0 & C & \vdots & 0 \\ \vdots & \vdots & \vdots & \vdots \\ 0 & 0 & \cdots & C \end{bmatrix} \begin{bmatrix} \hat{x}[k+1|k] \\ \hat{x}[k+2|k] \\ \vdots \\ \hat{x}[k+N_P|k] \end{bmatrix} \tag{2.11}$$

Equation (2.10) and (2.11) can be written as

$$X[k] = P_x \hat{x}[k|k] + P_u u[k-1] + P_{\Delta u} \Delta U[k] \tag{2.12}$$

$$Y[k] = P_y X[k] = P_y P_x \hat{x}[k|k] + P_y P_u u[k-1] + P_y P_{\Delta u} \Delta U[k] \tag{2.13}$$

where:

$$P_x = \begin{bmatrix} A \\ A^2 \\ \vdots \\ A^{N_P} \end{bmatrix} \qquad P_u = \begin{bmatrix} B \\ AB+B \\ \vdots \\ \sum_{i=0}^{N_P-1} A^i B \end{bmatrix} \qquad P_y = \begin{bmatrix} C & 0 & \cdots & 0 \\ 0 & C & \vdots & 0 \\ \vdots & \vdots & \vdots & \vdots \\ 0 & 0 & \cdots & C \end{bmatrix}$$

$$P_{\Delta u} = \begin{bmatrix} B & 0 & 0 \\ AB + B & B & 0 \\ \vdots & \vdots & 0 \\ \sum_{i=0}^{N_C-1} A^i B & \sum_{i=0}^{N_C-2} A^i B & \vdots \\ \vdots & \vdots & B \\ \sum_{i=0}^{N_P-1} A^i B & \sum_{i=0}^{N_P-2} A^i B & \vdots \\ & & \sum_{i=0}^{N_P-N_C} A^i B \end{bmatrix}$$

Based on the above prediction equations, the MPC seeks for an optimal sequence of $\hat{u}[k+i|k]$ which minimizes a given cost function. A typical cost function is given in Equation (2.14). It penalizes the deviation of the predicted controlled output $\hat{y}[k+i+1|k]$ from a reference trajectory $y_{ref}[k+i+1|k]$ and the input change $\Delta\hat{u}[k+i|k]$. The reference trajectory may be some predetermined trajectories.

$$J[k] = \sum_{i=0}^{N_P-1} \left\| \hat{y}[k+i+1|k] - y_{ref}[k+i+1|k] \right\|^2_{W_{y_i}} + \sum_{i=0}^{N_C-1} \|\Delta\hat{u}[k+i|k]\|^2_{W_{\Delta u_i}} \quad (2.14)$$

The prediction horizon has length N_P but is not necessary to start penalizing deviation of y from y_{ref} immediately because there may be some delay between applying an input and seeing any effect. W_{y_i} and $W_{\Delta u_i}$ are weight matrices. The solution minimizing Equation (2.14) should be subject to the following constraints:

$$E\ vec(\Delta\hat{u}[k|k], \dots, \Delta\hat{u}[k+N_C-1|k],1) \leq vec(0) \quad (2.15)$$

$$F\ vec(\hat{u}[k|k], \dots, \hat{u}[k+N_C-1|k],1) \leq vec(0) \quad (2.16)$$

$$G\ vec(\hat{y}[k+H_w|k], \dots, \hat{y}[k+N_P|k],1) \leq vec(0) \quad (2.17)$$

The constraints were assumed to hold over the control and prediction horizons. E, F and G are matrices of suitable dimensions. $vec(0)$ denotes a column vector, each of which is zero. These constraints can be used, for example, to represent possible actuator slew

rates (2.15), actuator ranges (2.16), and constraints on the controlled variables (2.17). When solving MPC optimization problem, all the above inequalities must be translated into the inequality concerning $\Delta\hat{u}[k+i|k]$, namely

$$E\ (\Delta\hat{u}[k|k], \Delta\hat{u}[k+1|k], \ldots, \Delta\hat{u}[k+N_P-1|k]) = E\Delta U[k] \leq e$$

Here, E is a coefficient matrix of proper dimensions.

2.5 Advantages and Disadvantages of MPC

MPC has the following main advantages [24]:

- Concepts are intuitive and attractive to industry
- Can be used to control a great variety of processes, including those with non-minimum phase, long time delay or open-loop unstable characteristics
- Can deal with multivariable, multi-input multi-output as well as single-input single-output process
- Constraints on inputs and outputs are considered in a systematic manner
- Readily applicable to batch processes where the future reference signals are known
- An open technology which allows for future extensions
- Accurate model predictions can provide early warning of potential problems

Significant disadvantages are:

- Requirement of an appropriate model of the process, which may be difficult to obtain for some complex systems
- Computationally demanding if the optimization problem is not formulated properly

2.7 MPC History and State of the Art

The MPC concept has a long history. Its current industrial and academic interest can be traced back to a set of papers which appeared in the late 1970s. In 1978 Richalet et al. [27] describes successful applications of "Model Predictive and Heuristic Control" and in 1979 engineers from Shell (Cutler and Ramaker [28]; Prett and Gillette [29]) outlined "Dynamic Matrix Control" and reported applications to a fluid catalytic cracker. In both algorithms an explicit dynamic model of the plant is used to predict the effect of future actions of the manipulated variables on the output (thus the name Model Predictive Control). The future moves of the manipulated variables are determined by optimization with the objective of minimizing the predicted error subject to operating constraints. The optimization is repeated at each sampling time based on updated information (measurements) from the plant.

Even though the above two works sparked the current interest in MPC, what have since become recognized as the central MPC concepts actually predates these first reports of application by some twenty years [30]. Zadeh and Whalen [31] first recognize the connection between the closely related minimum time optimal control problem and linear programming. The first publication to explicitly introduce the now standard MPC concept seems to be Propoi [32], who proposed in 1963 the moving horizon approach which is an essential part of all MPC algorithms. It became known as "Open Loop Optimal Feedback". During the 1970s, Gutman [33] reviewed much of the extensive work in this area. The connection between this work and MPC was discovered by Chang and Seborg [34].

Garcia and Morari [35] were perhaps the first to attempt placing the MPC within the same framework as the so-called "classical Control", in which the Internal Model Control (IMC) paradigm was proposed. They showed that the IMC structure – in which an internal model of the plant operates in parallel with the plant, and in which the controller is some appropriate inverse of this plant model – is inherent in all MPC scheme. This and subsequent publications by Morari and coworkers provided insight into the stability, robustness and performance of MPC scheme [36, 37].

Keyser et al. [38] presented a comparative study of self-adaptive long range predictive control (LRPC) technique while keeping focus on robustness with respect to unmodeled dynamics, parameter variations, process noise and varying dead-time. Scattolini and Bittanti [39] produce some simple criteria stated in terms of the plant step or impulse response for the selection of prediction horizon. This selection is important as it guarantees the closed-loop stability.

In 1991, Scattolini and Clarke [40] found that constrained receding horizon predictive control optimizes a quadratic function over a costing horizon to stabilize general linear plants. The computation is more complex, however. An alternative is to employ finite-horizon techniques, which are numerically very sensitive.

In 1999, Morari and Bemporad [41] investigate robustness in MPC and proposed techniques for stability, performance and constraint handling. Joe Qin and Badgwell [42] came up with an overview of commercially available MPC technology. They reported wide application of MPC in industrial applications.

Nonlinear MPC based on state space models and the receding horizon concept has also been developed, for example by Mayne and Michalska [43], who perform a stability analysis, and Balchen, Ljungquist and Strand [44]. Becerra, Roberts and Griffiths [45] integrate an economic objective within the performance function.

In 2007, Dubay and Ayyad [46] provided real time comparison of a number of predictive controllers.

2.8 Review of MPC Applications in Power Systems

MPC presents a dramatic advancement in the theory of modern automatic control [47]. It was originally studied and applied in the process industry, where it has been in use for decades [48]. An MPC survey by Qin and Badgwell [42] reported that there were over 4,500 applications worldwide by the end of 1999, primarily in oil refineries and petrochemical plants. In these industries, MPC has become the method of choice for difficult multivariable control problems that include inequality constraints.

In view of its remarkable success, a question to be answered is, why is MPC, hitherto, not extensively applied to control other systems, such as electrical power systems? This is as a result of two short comings. First, MPC needs an accurate model of the system, and this is not usually a simple task. Secondly, computational burden of MPC increases exponentially. These shortcomings were, however, solved as a result of availability of very good mathematical models and powerful microprocessors that can perform the large amount of computations needed in MPC at a high speed and reduced cost.

These advancements lead to a growing application of MPC in other areas. In the field of power systems, for example, it finds applications in power electronics [49, 50, 51], frequency control [52, 53], voltage control [54, 55], power system transient stability [56, 57], power system protection [58, 59], and smart-grids [60, 61], among others.

In recent years, MPC is extensively employed by researchers to design wide-area damping controller to damp out inter-area oscillations in power system.

Paper [62] introduces a new MPC scheme to damp wide-area electromechanical oscillations in power system. The proposed MPC controller, based on a linearized discrete-time state space model, calculates the optimal input sequence for local damping controllers over a chosen time horizon by solving a quadratic programming problem.

Distributed Model Predictive Control was investigated in reference [63] to damp wide-area electromechanical oscillations. This distributed MPC scheme is derived from and compared with a fully centralized MPC scheme proposed in [62].

An efficient adaptive stability control for multi-generator power system is presented in [64] based on step-ahead model prediction methodology. Method of Equivalent Circuit (MEC) is proposed to design the Model Predictive Adaptive Controller (MPAC) excitation for multi-generator power system by defining the deviation of predicted output from reference and control input increment as an objective function

In [65], a wide-area damping supplementary inter-area controller, using the reduced order state space model with dominant low frequency oscillations modes obtained by

system identification, based on model prediction and sliding mode variable structure control, was designed to damp the inter-area low frequency oscillations in power system.

CHAPTER 3

MPC WIDE-AREA DAMPING CONTROL DESIGN

3.1 Introduction

This chapter presents the design methodology of wide-area MPC damping controller. The following are the steps taken in the design proposed in this thesis:

Step 1. Full-order nonlinear model of the test system: The multi-machine dynamic model of the test system is calculated using Power System Toolbox [66]. All generators are represented by the detail model, i.e. two-axis model with exciter, governor and conventional power system stabilizers.

Step 2. Model linearization: The full-order nonlinear model is linearized at a chosen operating point. This is necessary since the proposed MPC controller requires a linear model for its predictions.

Step 3. Modal analysis and small signal stability: Once the linearized model of the system is obtained, the small signal stability analysis can be computed and analyzed. The eigenvalues and eigenvectors are determined to get the frequencies and damping ratios of local and inter-area modes.

Step 4. Controller Synthesis: An MPC technique is used to calculate the optimal input sequence and send these signals to each generator excitation system. MATLAB MPC Toolbox is used to design the controller. The designed controller should meet the requirement of stability and provide acceptable damping to inter-area oscillations.

Step 5. Simulation and results: The performance of the controller is evaluated in the closed-loop system with the full-order linear model using MATLAB.

3.2 MPC Wide-Area Damping Controller Architecture

The architecture of the proposed MPC wide-area damping controller is illustrated in Fig3.1. In most power systems, local oscillation modes are often well damped due to the installation of local PSS. Inter-area oscillation modes, on the other hand, are often lightly damped because the control inputs used by those PSS are local signals which often lack good observation of inter-area modes. This suggests that a wide-area controller, which uses wide-area measurements as its inputs to create control signals supplement to local PSSs, may help to improve the damping of inter-area oscillations.

In real time, the wide-area MPC controller collects WAMS measurements measured by PMUs and sent to the MPC controller via dedicated communication link (WAMS). These measurements, $\hat{x}[t]$ of the system state (a state estimator would normally be needed) are collected at discrete measurement times Δt (in this thesis $\Delta t = 0.1s$). The MPC uses its model to compute an open loop sequence of the control variables u over a chosen control horizon N_C. It sends these control signals computed for the first period of Δt seconds to the excitation system of each generator. It then waits for the next measurements to be received in order to start this calculation again.

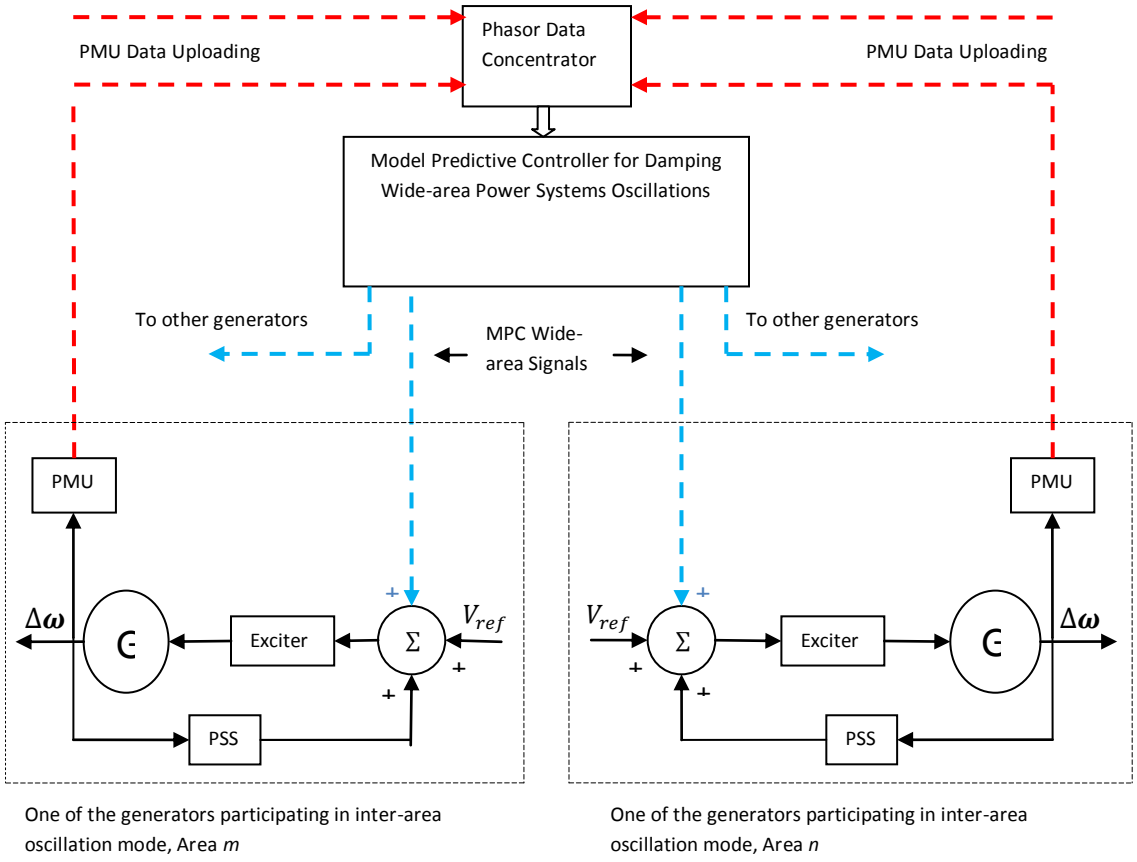

Fig. 3.1 Architecture of MPC Wide-area Damping Control Systems

3.3 Power System Modeling

In power systems, the primary sources of electrical energy are synchronous generators. The stability of the system depends on several other components such as excitation systems, speed governors, power system stabilizers, the loads etc. Therefore, an understanding of their characteristics and modeling of their performance are of fundamental importance for stability studies and control design. The general approach to modeling these components are quite standard. This section provides the detail of power system dynamic model used in this thesis.

3.3.1 Synchronous Generator Model

Synchronous generators form the principal source of electric energy in power system. The power system stability problem is largely one of keeping interconnected synchronous machines in synchronism. In this thesis, a sixth-order subtransient model, as described in [67] has been used.

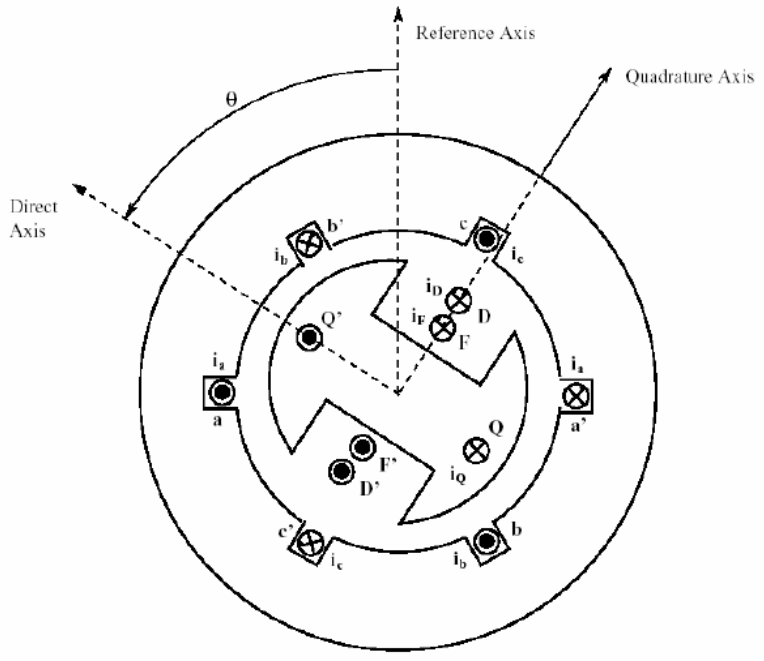

Fig. 3.2 Synchronous Generator Schematic Diagram

The six dynamic equations that model the sixth-order subtransient synchronous generator in Fig. 3.2 can be stated as:

$$\dot{\delta} = \Delta\omega \tag{3.1}$$

$$J\dot{\omega} = T_m - T_e - \widehat{D}\Delta\omega \tag{3.2}$$

$$T_{do}^{'}\dot{E}_q^{'} = -E_q^{'} - \left(X_d - X_d^{'}\right)$$

$$\left[I_d - \frac{X_d^{'} - X_d^{'}}{\left(X_d^{'} - X_{ls}\right)^2}\left(\psi_{1d} + \left(X_d^{'} - X_{ls}\right)I_d - E_q^{'}\right)\right] + E_{fd} \quad (3.3)$$

$$T_{qo}^{'}\dot{E}_d^{'} = -E_d^{'} - \left(X_q - X_q^{'}\right)$$

$$\left[I_q - \frac{X_q^{'} - X_q^{'}}{\left(X_q^{'} - X_{ls}\right)^2}\left(\psi_{2q} + \left(X_q^{'} - X_{ls}\right)I_q - E_d^{'}\right)\right] \quad (3.4)$$

$$\psi_d^{''} = \frac{E_q^{'}\left(X_d^{''} - X_l\right) + \psi_{1d}\left(X_d^{'} - X_d^{''}\right)}{X_d^{'} - X_l} - X_d^{''}I_d \quad (3.5)$$

$$\psi_q^{''} = \frac{E_d^{'}\left(X_q^{''} - X_l\right) + \psi_{1q}\left(X_q^{'} - X_q^{''}\right)}{X_q^{'} - X_l} - X_q^{''}I_q \quad (3.6)$$

where

δ	generator rotor angle
ω	generator rotor speed in per unit
J	moment of inertia
T_m	mechanical torque
T_e	electromechanical torque
$\widehat{D}$	damping coefficient
$\psi_d^{''}, \psi_q^{''}$	direct and quadrature axis components of stator flux linkage
$E_d^{'}, E_q^{'}$	direct and quadrature axis transient stator voltage
ψ_{1d}, ψ_{1q}	direct and quadrature armortisseur circuit flux linkage
X_l	leakage reactance;
$X_d, X_d^{'}, X_d^{''}$	direct axis synchronous, transient and subtransient reactances;
$X_q, X_q^{'}, X_q^{''}$	quadrature axis synchronous, transient and subtransient reactances;

T'_{qo}, T''_{qo} quadrature axis open circuit and subtansient time constants;

I_d, I_q direct and quadrature axix stator current

E_{fd}, I_{fd} excitation voltage and current

3.3.2 Exciter Model

When the behavior of synchronous machines is to be accurately simulated in power system stability studies, it is essential that their excitation systems be modeled in sufficient detail [68]. The basic function of an excitation system is to provide direct current to the synchronous machine field winding. In addition, the excitation system performs control and protective functions essential to the satisfactory performance of the power system by controlling the field voltage and thereby the field current. The desired models must be suitable for representing the actual excitation equipment performance for large, severe disturbances as well as for small perturbations.

IEEE Type DC1A Exciter [69] is used in this thesis. Its block diagram is shown in Fig. 3.3.

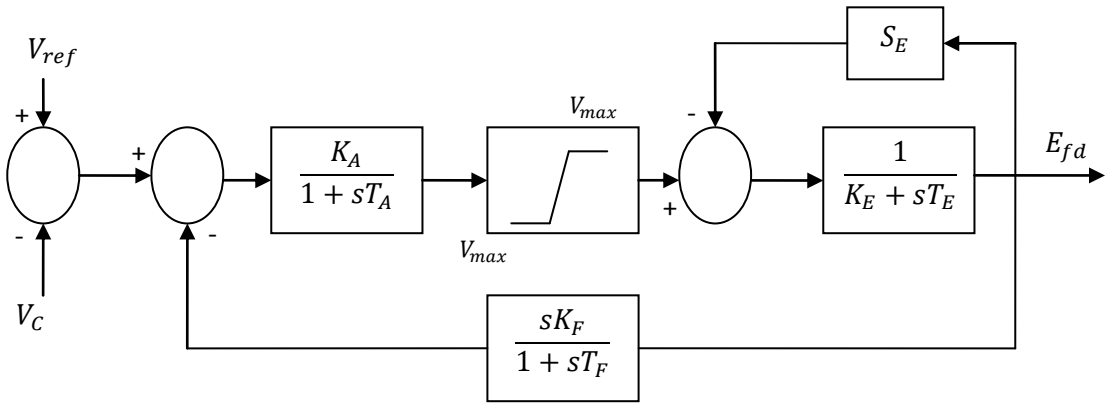

Fig. 3.3 IEEE DC1A Exciter Block Diagram [69]

The dynamics of this exciter can be represented by the following differential equations:

$$\dot{V}_{AS} = \frac{V_{err} - V_{As}}{T_b} \tag{3.7}$$

$$V_A = \frac{T_c}{T_b} V_{err} + (1 - \frac{T_c}{T_b}) V_{As} \tag{3.8}$$

$$\dot{E}_{fd} = \frac{K_a V_A + E_{fd}}{T_a} \tag{3.9}$$

where

V_{err}	voltage deviation
V_{ref}	exciter reference voltage
$V_{As,} V_A$	regulator states
K_a	voltage regulator gain
T_a	voltage regulator time constant
T_b, T_c	transient gain reduction time constants

3.3.3 Governor Model

The prime mover governing systems provide a means of controlling the synchronous machine speed and hence voltage frequency. In order to automatically control speed and frequency, a device must sense either speed or frequency in such a way that comparison with a desired value can be used to create an error signal to take corrective action.

$$\dot{TG}_1 = \frac{(TG_{in} - TG_1)}{T_s} \tag{3.10}$$

$$\dot{TG}_2 = \frac{(1 - \frac{T_3}{T_c}) TG_1 - TG_2)}{T_c} \tag{3.11}$$

$$\dot{TG}_3 = \frac{\left(TG_2 + \frac{T_3}{T_c} TG_1\right)(1 - \frac{T_4}{T_5}) - TG_3}{T_5} \tag{3.12}$$

$$P_m = TG_3 + \frac{T_4}{T_5}(TG_2 + \frac{T_3}{T_C} TG_1) \tag{3.13}$$

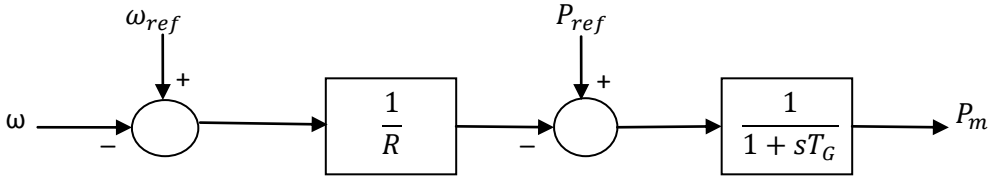

Fig. 3.4 Governor Model Block Diagram [67]

3.3.4 Power System Stabilizer Model

The basic function of Power System Stabilizer (PSS) is to add damping to the generator rotor oscillations by controlling its excitation using auxiliary stabilizing signal(s). To provide damping, the stabilizer must produce a component of electrical torque in phase with the rotor speed deviations. Fig. 3.5 illustrates the theoretical basis for a PSS with the help of block diagram. Since the purpose of a PSS is to introduce damping torque component, a logical signal to use for controlling generator excitation is the speed deviation.

$$\dot{V}_w = -\frac{T_w\dot{\omega}-V_w}{T_w} \tag{3.14}$$

$$\dot{V}_1 = \frac{\left(1-\frac{T_{n1}}{T_{d1}}\right)K_{pss}\dot{V}_w-V_1}{T_{d1}} \tag{3.15}$$

$$\dot{V}_2 = \frac{\left(1-\frac{T_{n2}}{T_{d2}}\right)\dot{V}_1-V_2}{T_{d2}} \tag{3.16}$$

$$V_{pss} = \frac{T_{n2}}{T_{d2}}\left(\frac{T_{n1}}{T_{d1}}K_{pss}\dot{V}_w + V_1\right) + V_2 \tag{3.17}$$

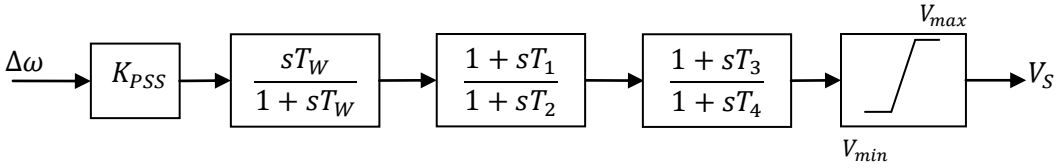

Fig. 3.5 Power System Stabilizer Model Block Diagram [69]

3.3.5 Load Model

Modeling load in stability studies is complicated because a typical load bus is composed of a large number of devices such as fluorescent and incandescent lamps, refrigerators, heaters, compressors, motors, furnaces, etc. Therefore, load representation in system studies is based on a considerable amount of simplification.

Load can be either static or dynamic and can be modeled using constant impedance, constant current and constant power static load models. These loads can be described by the following polynomial equations [70]:

$$P_L = kP_0\left[A_1 + A_2\frac{V}{V_0} + A_3\left(\frac{V}{V_0}\right)^2\right] \tag{3.18}$$

$$Q_L = kQ_0\left[B_1 + B_2\frac{V}{V_0} + B_3\left(\frac{V}{V_0}\right)^2\right] \tag{3.19}$$

where $A_1 + A_2 + A_3 = B_1 + B_2 + B_3 = 1$; P_0 and Q_0 are the load real and reactive powers consumed under nominal conditions, i.e., at the reference voltage V_0 and the nominal frequency f_0. P_L and Q_L are the powers consumed by the load under current conditions of voltage V and frequency f. The value k is a loading factor, which is an independent demand variable.

3.4 Linearized State Space Model of Power System

Although a real power system is a complex, nonlinear and high-order dynamic system, it can be represented by a relatively simple linear model with fixed structure but whose parameters vary with the operating conditions, which is accurate enough for the purpose of designing a damping controller.

The synchronous generator model along with the associated regulating devices thus becomes a fifteenth-order model (15 state variables for each synchronous machine). These dynamic states are:

6 Generator states: $\delta,\quad \Delta\omega,\quad E'_d,\quad E'_d,\quad \psi''_d,\quad \psi''_d$

3 Exciter states: V_{AS}, V_A, E_{fd}

3 Governor states: tg_1, tg_2, tg_3

3 PSS states: V_w, V_1, V_2

The states vector is thus;

$$x = [\delta \quad \Delta\omega \quad E'_d \quad E'_d \quad \psi''_d \quad \psi''_d \quad V_{AS} \quad V_A \quad E_{fd} \quad tg_1 \quad tg_2 \quad tg_3 \quad V_w \quad V_1 \quad V_2]^T$$

In the design proposed in this thesis, the control inputs to the power system are additional MPC wide-area signals added to each generator excitation system. The control inputs are:

$$u = [u_1 \quad u_2 \quad u_3 \ldots u_{ng}]$$

where *ng* is the number of controlled generators.

The 15 differential equations describing each machine are:

$$\dot{\delta} = \Delta\omega$$

$$J\dot{\omega} = T_m - T_e - \widehat{D}\Delta\omega$$

$$T'_{do}\dot{E}'_q = -E'_q - \left(X_d - X'_d\right)$$

$$\left[I_d - \frac{X'_d - X'_d}{\left(X'_d - X_{ls}\right)^2}\left(\psi_{1d} + \left(X'_d - X_{ls}\right)I_d - E'_q\right)\right] + E_{fd}$$

$$T'_{qo}\dot{E}'_d = -E'_d - \left(X_q - X'_q\right)$$

$$\left[I_q - \frac{X'_q - X'_q}{\left(X'_q - X_{ls}\right)^2}\left(\psi_{2q} + \left(X'_q - X_{ls}\right)I_q - E'_d\right)\right]$$

$$\psi''_d = \frac{E'_q\left(X''_d - X_l\right) + \psi_{1d}\left(X'_d - X''_d\right)}{X'_d - X_l} - X''_d I_d$$

$$\psi_q^{''} = \frac{E_d^{'}(X_q^{''} - X_l) + \psi_{1q}(X_q^{'} - X_q^{''})}{X_q^{'} - X_l} - X_q^{''} I_q$$

$$\dot{V}_{AS} = \frac{V_{err} - V_{As}}{T_b}$$

$$V_A = \frac{T_c}{T_b} V_{err} + (1 - \frac{T_c}{T_b}) V_{As}$$

$$\dot{E}_{fd} = \frac{K_a V_A + E_{fd}}{T_a}$$

$$\dot{TG}_1 = \frac{(TG_{in} - TG_1)}{T_s}$$

$$\dot{TG}_2 = \frac{(1 - \frac{T_3}{T_c}) TG_1 - TG_2)}{T_c}$$

$$\dot{TG}_3 = \frac{\left(TG_2 + \frac{T_3}{T_c} TG_1\right)(1 - \frac{T_4}{T_5}) - TG_3}{T_5}$$

$$\dot{V}_w = -\frac{T_w \dot{\omega} - V_w}{T_w}$$

$$\dot{V}_1 = \frac{\left(1 - \frac{T_{n1}}{T_{d1}}\right) K_{pss} \dot{V}_w - V_1}{T_{d1}}$$

$$\dot{V}_2 = \frac{\left(1 - \frac{T_{n2}}{T_{d2}}\right) \dot{V}_1 - V_2}{T_{d2}}$$

The full dynamic behavior of the power system may be describe by a set of first order nonlinear differential equations as presented below

$$\dot{x} = f(x, u, t) \tag{3.20}$$

If the derivatives of the state variables are not explicit function of time, the system is said to be autonomous. In this case, Equation 3.20 simplifies to

$$\dot{x} = f(x, u) \tag{3.21}$$

Often, the variables of interest are output variables which can be observed on the system. These may be expressed in terms of the state variables and the output variables in the following form:

$$y = g(x, u) \tag{3.22}$$

Let x_0 be the initial state vector and u_0 the input vector corresponding to the equilibrium point about which the small-signal performance is to be investigated. Since x_0 and u_0 satisfy Equation 3.21, then

$$\dot{X}_0 = f(X_0, U_0) = 0 \tag{3.23}$$

Let's perturb the system from the above state, by letting

$$X = X_0 + \Delta X \qquad\qquad U = U_0 + \Delta U$$

prefix Δ denotes a small deviation.

The new state must satisfy Equation 3.21. Hence,

$$\dot{X} = \dot{X}_0 + \Delta X_0 = f[(X_0 + \Delta X), (U_0 + \Delta U) \tag{3.24}$$

As the perturbations are assumed to be small, the nonlinear function $f(x, u)$ can be expressed in terms of Taylor's series expansion. All the terms involving second and higher order powers of Δx and Δu are neglected, it can be written:

$$\dot{x}_i = \dot{x}_{i0} + \Delta\dot{x}_i = f_i[(X_0 + \Delta X), (U_0 + \Delta U)]$$

$$= f_i(X_0, U_0) + \frac{\partial f_i}{\partial x_i}\Delta x_i + \cdots + \frac{\partial f_i}{\partial x_n}\Delta x_n + \frac{\partial f_i}{\partial u_1}\Delta u_1 + \cdots + \frac{\partial f_i}{\partial u_r}\Delta u_r$$

Since $\dot{x}_{i0} = f_i(X_0, U_0)$, we obtain

$$\Delta\dot{x}_i = \frac{\partial f_i}{\partial x_1}\Delta x_1 + \cdots + \frac{\partial f_i}{\partial x_n}\Delta x_n + \frac{\partial f_i}{\partial u_1}\Delta u_1 + \cdots + \frac{\partial f_i}{\partial u_r}\Delta u_r$$

With $i = 1, 2, 3, \ldots, n$. In a like manner, from Equation (3.22), it can be expressed:

$$\Delta y_j = \frac{\partial g_j}{\partial x_1}\Delta x_1 + \cdots + \frac{\partial g_j}{\partial x_n}\Delta x_n + \frac{\partial g_j}{\partial u_1}\Delta u_1 + \cdots + \frac{\partial g_j}{\partial u_r}\Delta u_r$$

With $j = 1, 2, 3, \dots, m$. Therefore, the linearized forms of Equations (3.21) and (3.22) are

$$\Delta\dot{X} = A\Delta X + B\Delta U \tag{3.25}$$

$$\Delta y = C\Delta X + D\Delta U \tag{3.26}$$

where

$$A = \begin{bmatrix} \frac{\partial f_1}{\partial x_1} & \cdots & \frac{\partial f_1}{\partial x_n} \\ \cdots & \cdots & \cdots \\ \frac{\partial f_n}{\partial x_1} & \cdots & \frac{\partial f_n}{\partial x_n} \end{bmatrix} \qquad B = \begin{bmatrix} \frac{\partial f_1}{\partial u_1} & \cdots & \frac{\partial f_1}{\partial u_r} \\ \cdots & \cdots & \cdots \\ \frac{\partial f_n}{\partial u_1} & \cdots & \frac{\partial f_n}{\partial u_r} \end{bmatrix}$$

$$C = \begin{bmatrix} \frac{\partial g_1}{\partial x_1} & \cdots & \frac{\partial g_1}{\partial x_n} \\ \cdots & \cdots & \cdots \\ \frac{\partial g_m}{\partial x_1} & \cdots & \frac{\partial g_m}{\partial x_n} \end{bmatrix} \qquad D = \begin{bmatrix} \frac{\partial g_1}{\partial u_1} & \cdots & \frac{\partial g_1}{\partial u_r} \\ \cdots & \cdots & \cdots \\ \frac{\partial g_m}{\partial u_1} & \cdots & \frac{\partial g_m}{\partial u_r} \end{bmatrix}$$

The above partial derivatives are evaluated at the equilibrium point about which the small perturbation is being analyzed.

3.5 Modal Analysis and Small Signal Stability

Small signal stability of the power system can be calculated and analyzed once the power system is represented in general state space form as given in (3.25) and (3.26). Because each eigenvalues correspond to an oscillation mode of the system, small signal stability analysis is also referred to as modal analysis [67].

Small signal analysis establishes that the stability of a system equilibrium point under small disturbances can be studied by linearizing the nonlinear system equation around the system equilibrium point. Then, the system stability can be determined by inspecting the eigenvalues, λ_i of the system state matrix A [71]. Eigenvalues are the non-trivial solutions of the equation:

$$A\phi = \lambda\phi \tag{3.27}$$

where ϕ is an $n \times 1$ vector. Rearranging (3.25) to solve for λ yields

$$\det(A - \lambda) = 0 \tag{3.28}$$

The solution of (3.28) are the eigenvalues of the $n \times n$ matrix of A. These eigenvalues are of the form $\sigma \pm j\omega$. The operating point is stable if all the eigenvalues are on the left-hand side of the imaginary axis of the complex plane; otherwise it is unstable. As a pair of complex eigenvalues crosses the imaginary axis, it is known as Hopf bifurcation [72].

The oscillation frequency in Hertz and damping ratio are given by:

$$f = \frac{\omega}{2\pi} \tag{3.29}$$

$$\xi = \frac{-\sigma}{\sqrt{\sigma^2 + \omega^2}} \tag{3.30}$$

In linear system, the dynamics can be described as a collection of modes. A mode is characterized by its frequency and damping and the activity pattern of the system states.

The system matrix A can be diagonalized by the square right modal matrix ϕ:

$$\phi^{-1} A \phi = \Lambda \tag{3.31}$$

The columns of ϕ are the right eigenvector ϕ_i to A, while the diagonal elements of the diagonal matrix Λ are the eigenvalues λ_i of A. Similarly the left modal matrix ψ holds the left eigenvector ψ_i as rows and also diagonalizes A.

$$\psi A \psi^{-1} = \Lambda \tag{3.32}$$

The right and left modal matrix are normalized so that:

$$\psi \phi = I \tag{3.33}$$

The right eigenvector Φ_i gives the mode shape, i.e., the relative activity of the state variables when a particular mode is excited. Its magnitude give the extent of the activities of the *n* state variables in the *i*th mode, and the angles of the elements give phase displacements of the state variables displays only the *i*th mode. The left

eigenvector ψ_i identifies which combination of the original state variables displays only the *i*th mode.

3.6 Controller Synthesis

In this thesis, the real power system is replaced by nonlinear time domain simulation software, *s_simu*, from the MATLAB Power System Toolbox (PST) [66]. Next, *svm_mgen*, which is a small signal stability analysis software also from PST, is used to derive the linearized continuous time model

$$\dot{x} = A_C x + B_c u \tag{3.34}$$

$$y = C_C x \tag{3.35}$$

Where, $x \in R^{m_x}$ is a vector of state variables, $u \in R^{m_u}$ is vector of inputs, $y \in R^{m_y}$ is a vector of outputs. The Equation (3.34) and (3.35) were then discretized using a transition for a small step of δ seconds to obtain a discrete-time dynamics

$$x[k+1] = Ax[k] + Bu[k] \tag{3.36}$$

$$y[k] = Cx[k] \tag{3.37}$$

At time *t*, based on an estimation $\hat{x}(t)$ of the current system states (obtained from a state estimator), the predicted outputs $\hat{y}[k]$ over the next horizon are obtained by iterating Equation (3.36) and (3.37) N_P times by using $\hat{x}(t)$ as the initial state. N_P is the prediction horizon.

$$X[k] = P_x \hat{x}[k|k] + P_u u[k-1] + P_{\Delta u} \Delta U[k] \tag{3.38}$$

$$Y[k] = P_y X[k] = P_y P_x \hat{x}[k|k] + P_y P_u u[k-1] + P_y P_{\Delta u} \Delta U[k] \tag{3.39}$$

where:

$$P_x = \begin{bmatrix} A \\ A^2 \\ \vdots \\ A^{N_P} \end{bmatrix} \qquad P_u = \begin{bmatrix} B \\ AB + B \\ \vdots \\ \sum_{i=0}^{N_P-1} A^i B \end{bmatrix} \qquad P_y = \begin{bmatrix} C & 0 & \dots & 0 \\ 0 & C & \vdots & 0 \\ \vdots & \vdots & \vdots & \vdots \\ 0 & 0 & \dots & C \end{bmatrix}$$

$$P_{\Delta u} = \begin{bmatrix} B & 0 & 0 \\ AB + B & B & 0 \\ \vdots & \vdots & \vdots \\ \sum_{i=0}^{N_C-1} A^i B & \sum_{i=0}^{N_C-2} A^i B & B \\ \vdots & \vdots & \vdots \\ \sum_{i=0}^{N_P-1} A^i B & \sum_{i=0}^{N_P-2} A^i B & \sum_{i=0}^{N_P-N_C} A^i B \end{bmatrix}$$

Based on the above prediction equations, the MPC seeks for an optimal sequence of $\hat{u}[k+i|k]$ which minimizes a given cost function. A typical cost function is given in Equation (3.40). It penalizes the deviation of the predicted controlled output $\hat{y}[k+i+1|k]$ from a reference trajectory $y_{ref}[k+i+1|k]$ and the input change $\Delta\hat{u}[k+i|k]$. The reference trajectory may be some predetermined trajectories:

$$J[k] = \sum_{i=0}^{N_p-1} \left\| \hat{y}[k+i+1|k] - y_{ref}[k+i+1|k] \right\|^2_{W_{y_i}} + \sum_{i=0}^{N_C-1} \|\Delta\hat{u}[k+i|k]\|^2_{W_{\Delta u}} \quad (3.40)$$

The MATLAB MPC Toolbox is used to compute the solution of this quadratic programming problem. The first solution of this problem is sent to the excitation system of generators and the calculation is repeated at the next measurement step $k+i$ by using the measured state $\hat{x}(k+i)$ as input.

Controller Tuning

The following parameters need to be specified when designing MPC controller:

N_P: Prediction Horizon (number of predictions)

N_C: Control Horizon (number of control moves)

Δt: Sampling period

W_y: Weighting matrix for predicted errors ($W_y > 0$)

$W_{\Delta u}$: Weighting matrix for manipulated variables rate ($W_{\Delta u} \geq 0$)

W_u: Weighting matrix for manipulated variables($W_u \geq 0$)

Although the values of these parameters are normally guided by heuristics, there are some general guidelines for their selection to ensure the optimization is well proposed.

1. Choice of Horizons

   Prediction horizon, N_P

   Predictive horizon should be selected to include all significant dynamics; otherwise performance may be poor and important events may be unobserved. The prediction horizon should be larger than control horizon plus the system settling time.

   Control Horizon, N_C

   Increasing N_C makes the controller more aggressive and increases computational effort, typically

   $$5 \leq N_C \leq 20$$

   The control horizon should be as large as the expected transient behavior.

   Rossiter [25] summarizes the effects of varying these parameters:

   - If N_c is small, increasing N_P causes the loop dynamics to slow down
   - If N_c is large, increasing N_P improves performances
   - If N_P is large, then increasing N_c improves performance
   - If N_P is small, then increasing N_c can lead to near deadbeat behavior

- As N_P is increased, norminal closed-loop performance improves if N_c is large enough
- As N_c is increased nominal closed-loop performance improves if N_P is large enough. However, for many models, there is no much change beyond $N_c = 3$

2. Weighting matrices W_y, W_u and $W_{\Delta u}$

   Choosing the weights is a critical step in MPC [73]. Usually, the controller weights needs to be tune in order to achieve the desired behavior. Diagonal matrices with largest elements correspond to most important variables

   - Output weighting matrix W_y: the most important variables having the largest weights
   - Input weighing matrix (move suppression matrix) $W_{\Delta u}$: increasing the values of weights tend to make the MPC controller more conservative by reducing the magnitudes of the input moves. Increasing $W_{\Delta u}$ slows down the responses

CHAPTER 4

CASE STUDIES

4.1 Introduction

Inter-area oscillations in large interconnected systems are complex. There are generally many such modes, each involving a large number of generators. The complexity of the system models necessary to determine the stability of specific power obscures the fundamental nature of inter-area modes. Therefore, in order to be able to concentrate on those factors which affect inter-area modes, a simple hypothetical test system, IEEE 4-Generator 2-Area Test System, is constructed in [3]. The system is shown in Figure 4.1 and has both inter-area and local modes. Although small, the system parameters, and structure, are realistic.

Next, a larger and more complex system, IEEE 16-Generator 5-Area test system is constructed in [2]. These two test systems were selected as the benchmark systems for evaluating the performance of the proposed MPC wide-area damping controller.

4.2 IEEE 4-Generator 2-Area Test System

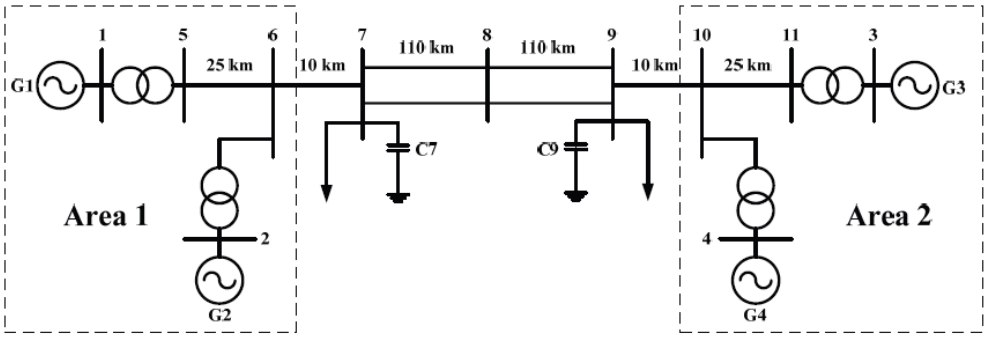

Fig. 4.1 IEEE 4-Generator 2-Areas Test System [3]

4.2.1 Test System Description

This system, shown in Fig. 4.1, was created to exhibit the different types of oscillations that occur in both large and small interconnected power systems. The base system is symmetric; it consists of two identical areas connected through a relatively weak tie. Each area includes two generating units, each having a rating of 900 MVA and 20 kV. The loads are at bus 7 in area 1, and at bus 9 in area 2. Bus 1 is assign as a swing bus. Each of the four generators is equipped with static exciter, turbine/governor, and local PSS. The system is operating with area 1 exporting 400 MW to area 2. Dynamic data for the generators and excitation systems used in this case study are given in Appendix A.

4.2.2 Full-order Model and Small Signal Analysis

The non linear model is linearized around an operating point by *svm_mgen*. The MATLAB script file, *svm_mgen*, is a Power System Toolbox (PST) driver for small signal stability analysis which calls the models of the PST to

- Select a data file
- Perform a load flow
- Form a linearized model by perturbing each in turn
- Do a modal analysis of the system

The number of dynamic states in this model is 64; 60 for the generators and their controls (each generator has 15 states) and 4 for the active and reactive load modulation. After running *svm_mgen*, the small signal analysis shows that this system is stable since all the eigenvalues are in the left-hand side of the imaginary axis (except the theoretically zero eigenvalue). The eigenvalues, damping ratios and frequencies of the modes of all the 64 states are:

Mode	Right eigenvalues	Damping	Frequency	Comment
1	0.0000	1.0000	0	Theoritically zero eigenvalues
2	-0.0922	1.0000	0	
3	-0.1002 - 0.0000i	1.0000	0.0000	
4	-0.1002 + 0.0000i	1.0000	0.0000	
5	-0.1003	1.0000	0	
6	-0.1844	1.0000	0	
7	-0.1845 - 0.0001i	1.0000	0.0000	
8	-0.1845 + 0.0001i	1.0000	0.0000	
9	-0.1866	1.0000	0	
10	-0.1954	1.0000	0	
11	-0.1978	1.0000	0	
12	-0.1978	1.0000	0	
13	-0.5211 - 0.5082i	0.7159	0.0809	
14	-0.5211 + 0.5082i	0.7159	0.0809	
15	-0.3404 - 0.6595i	0.4587	0.1050	
16	-0.3404 + 0.6595i	0.4587	0.1050	
17	-0.5320 - 0.5189i	0.7159	0.0826	
18	-0.5320 + 0.5189i	0.7159	0.0826	
19	-1.1579	1.0000	0	
20	-0.7035 - 1.2838i	0.4806	0.2043	
21	-0.7035 + 1.2838i	0.4806	0.2043	
22	-1.4663	1.0000	0	
23	-1.5579	1.0000	0	
24	-0.5540 - 1.5977i	0.3276	0.2543	
25	-0.5540 + 1.5977i	0.3276	0.2543	
26	-1.9050	1.0000	0	
27	-1.9894	1.0000	0	
28	-1.9906	1.0000	0	
29	-2.3663	1.0000	0	
30	-2.3837	1.0000	0	
31	-3.1146	1.0000	0	
32	-3.3944	1.0000	0	
33	-0.0974 - 3.4026i	0.0286	0.5415	Lightly-damped inter-area Mode
34	-0.0974 + 3.4026i	0.0286	0.5415	Lightly-damped inter-area Mode
35	-4.6443	1.0000	0	
36	-4.6648	1.0000	0	
37	-0.4941 - 6.7788i	0.0727	1.0789	
38	-0.4941 + 6.7788i	0.0727	1.0789	
39	-0.5078 - 6.8357i	0.0741	1.0879	
40	-0.5078 + 6.8357i	0.0741	1.0879	
41	-10.0712	1.0000	0	
42	-10.0718	1.0000	0	
43	-10.0992	1.0000	0	
44	-10.1102	1.0000	0	
45	-19.1942	1.0000	0	
46	-19.1961	1.0000	0	
47	-19.3047	1.0000	0	
48	-19.3924	1.0000	0	
49	-20.0000	1.0000	0	
50	-20.0000	1.0000	0	
51	-20.0000	1.0000	0	
52	-20.0000	1.0000	0	
53	-28.9774	1.0000	0	
54	-30.2323	1.0000	0	
55	-33.6969	1.0000	0	
56	-34.8376	1.0000	0	
57	-36.0189	1.0000	0	
58	-36.2034	1.0000	0	
59	-37.1492	1.0000	0	
60	-37.2206	1.0000	0	
61	-50.0001 - 0.0000i	1.0000	0.0000	
62	-50.0001 + 0.0000i	1.0000	0.0000	
63	-50.0001	1.0000	0	
64	-50.0001	1.0000	0	

There is a lightly damped inter-area mode of $0.0974 \pm j3.4026$ with frequency of 0.5415 and damping ratio of 0.0286. Fig. 4.2 shows the plot of frequency against damping ratio of the system's modes.

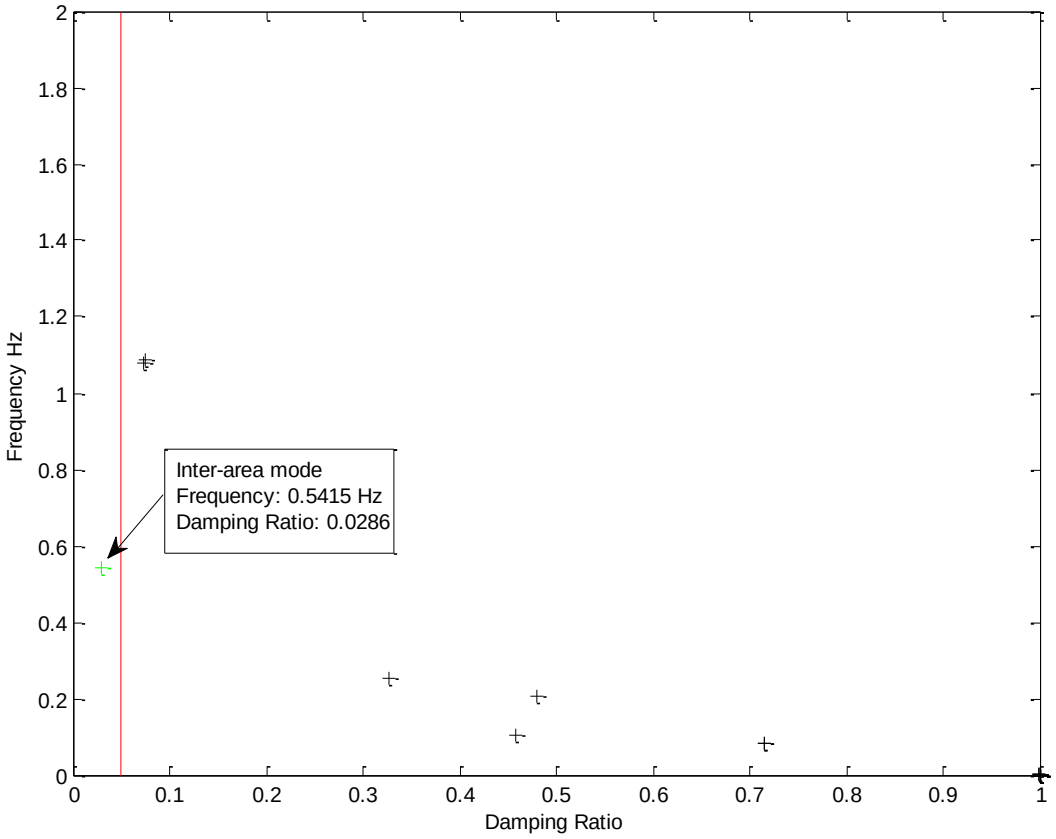

Fig. 4.2 Calculated Modes of IEEE 4-Generator 2-Area Test System

Mode shape and eigenvectors

The eigenvector associated with a mode indicates the relative change in the states which would be observed when the mode of oscillation is excited. Fig. 4.3 shows the compass plot of rotor angle terms of inter-area mode eigenvector. It enables us to confirm that mode 20 is an inter-area mode, since generators 1 and 2 are oscillating against generators 3 and 4.

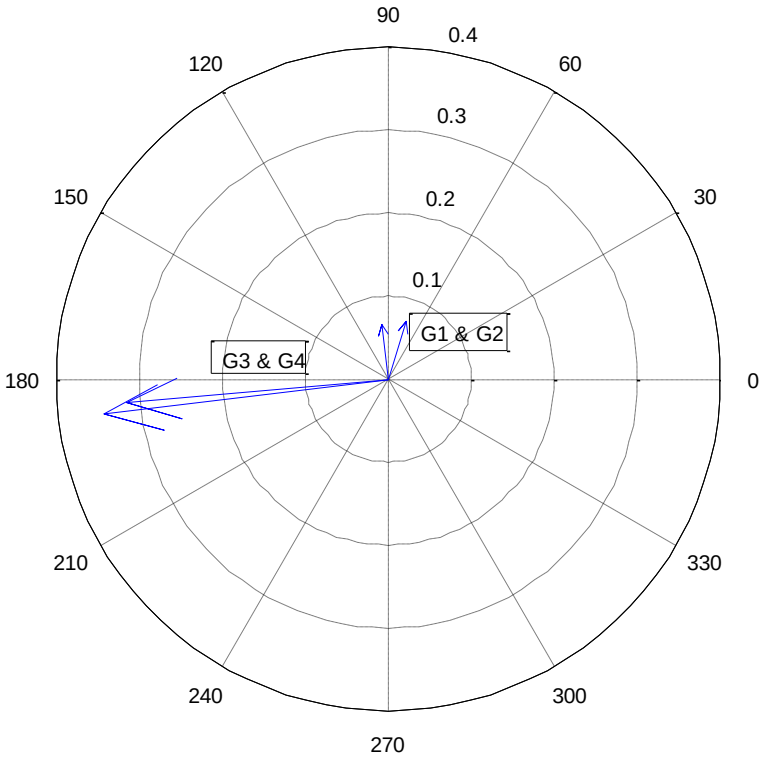

Fig. 4.3 Compass Plot of Rotor Angle Terms of Inter-area Mode Eigenvector

4.2.3 Structure of the proposed MPC Wide-area Damping Controller

The configuration of the generator equipped with the proposed MPC wide-area damping is shown in Fig. 4.4. The output of the local PSS, V_{PSS}, is used to provide damping for local modes using the rotor speed of the local generator as the input. All the local PSS are conventional controllers designed by classical methods. This results in a satisfactory damping of the local mode oscillations. To damp inter-area mode, local rotor speed of this generator is measured by PMU and sent to the MPC Wide-area damping controller as the input signal through Wide Area Measurement Systems (WAMS). The output control signal, u, of the MPC controller is then sent to the excitation system of all the generators to damp the inter-area oscillations.

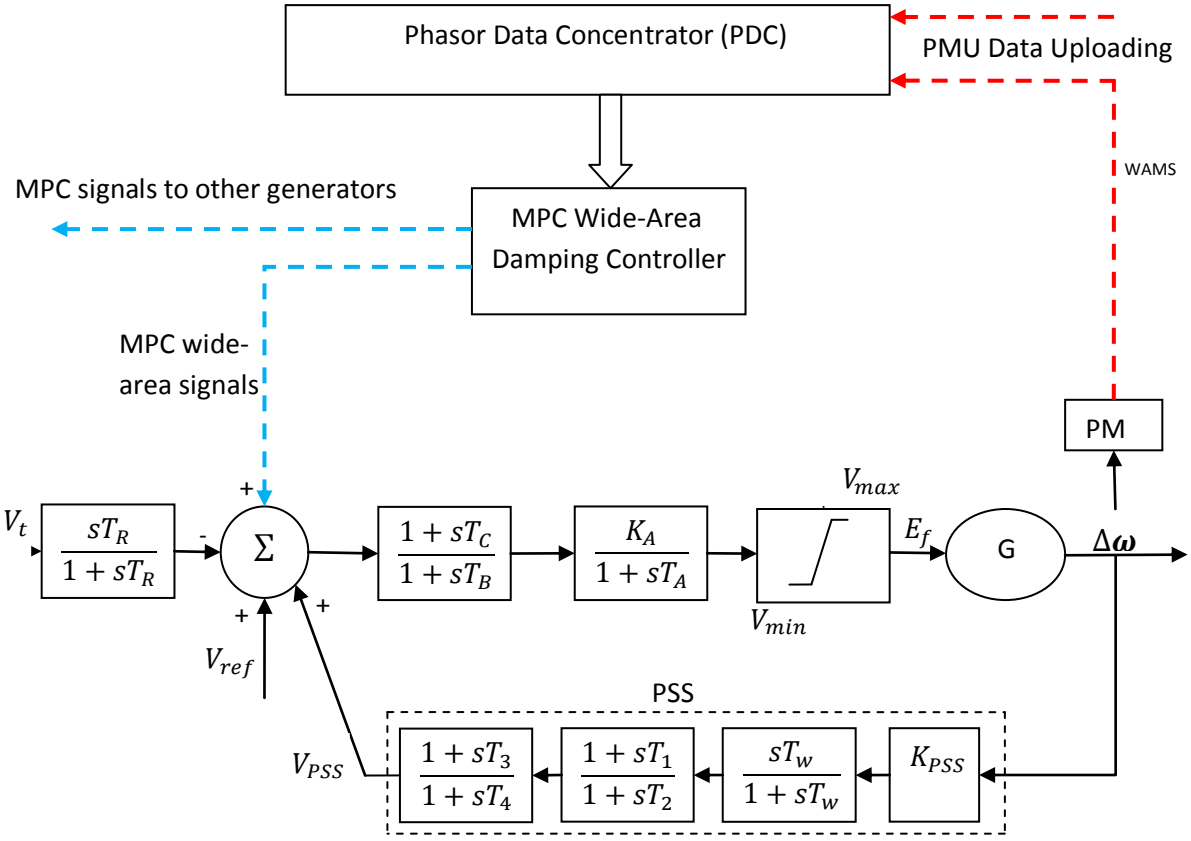

Fig. 4.4 Configuration of the generator participating in MPC wide-area damping

4.2.4 Control objectives and constraints

The small signal analysis performed by *svm_mgen* shows that this system has a lightly damped inter-area mode $0.0974 \pm j3.4026$ with frequency of 0.5415 Hz and damping ratio of 0.0286. The primary control objective of this MPC damping controller is aimed at achieving an acceptable damping for this mode.

Constraints are imposed on the control signal u as:

$$-0.1 \leq u \leq 0.1$$

These constraints were imposed on the MPC wide-area signal to avoid an excessive interference between wide-area damping control and the local control provided by PSS.

4.2.5 Controller Synthesis

The controller will be designed using MATLAB MPC Toolbox. The MPC state vector x contains 6×4 generator states, 3×4 exciter states, 3×4 PSS states, 3×4 turbine governor states. Output y is the vector of angular speeds, with reference y_{ref}, which is the unit vector of dimension 4. Input vector u consists of 4 MPC wide-area control signals to the excitation system of each generator.

- Controller Tuning

The following parameters need to be specified when designing MPC controller: Prediction Horizon (N_P), Control Horizon (N_C), Weights ($W_y W_{\Delta u}$), and Sampling Period, Δt.

Although the values of these parameters are normally guided by heuristics, there are some general guidelines for their selection to ensure satisfactory closed-loop performance and well-posed optimization.

Prediction and Control Horizons

For the proposed MPC controller, desired response can be achieved by setting:

Prediction horizon, $N_P = 100$

Control Horizon, $N_C = 10$

Weights

The following weights were found to provide a satisfactory performance.

Weights on manipulated variables, W_u = 0

Weights on manipulated variable rates, $W_{\Delta u}$ = 0.1

Weights on the output signal, W_y = 1

Sampling Interval

Sampling interval, Δt = 0.1

4.2.6 Simulation and Results

In order to fully test the effectiveness of the proposed MPC wide-area damping controller, the following disturbance is considered:

- Simulation scenario: An impulse signal at the input mechanical torque of generator 3

In this case scenario, the disturbance used is an impulse signal applied to the input mechanical torque of generator 3 (Fig. 4.1) in order to excite the inter-area oscillations. The time response of linear closed-loop system is used to verify the performance of the controller. Note that the disturbance is applied at $t = 1\ second$, because it is a good practice to run a simulation for a short time before applying a disturbance as this checks that the system has a satisfactory, stable initial conditions. Fig. 4.5 shows the simulated responses for this command over a period of 25s. When no MPC wide-area controller is used, sustained, slowly damped oscillations were observed.

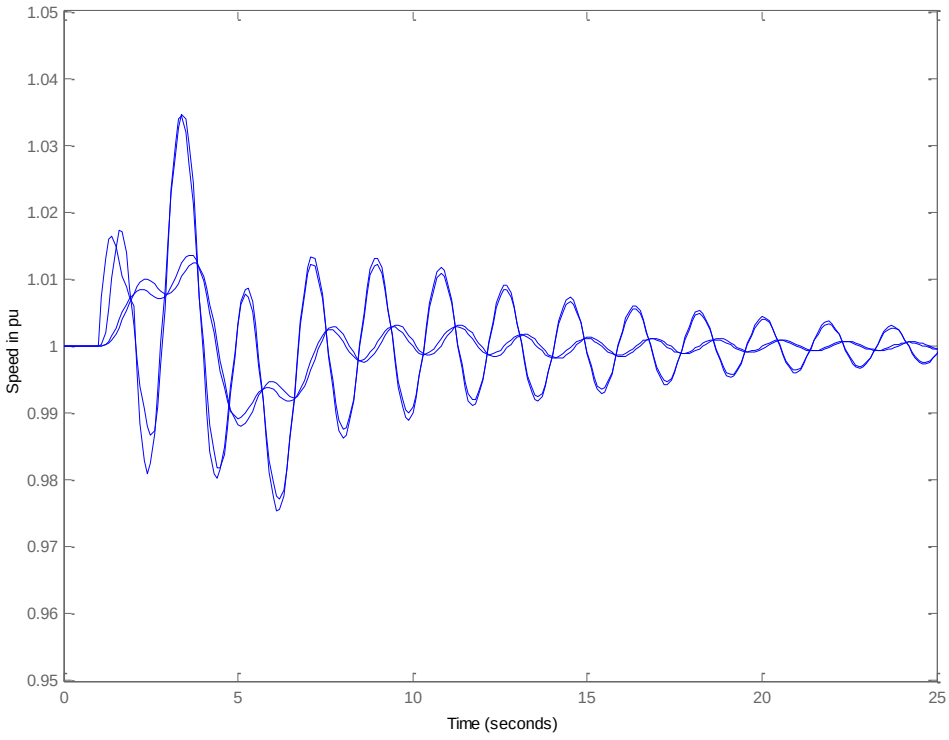

Fig. 4.5 Speeds of all 4 generators with only PSS (No MPC controller)

Next the MPC wide-area is introduced; Fig. 4.6 shows a response over a period of 25s. Compared with the system response without MPC controller (Fig. 4.5), it is observed that MPC wide-area damping controller damps the inter-area oscillations efficiently (Settling time is reduced to approximately 10 seconds). Fig 4.7 shows the control signals computed by MPC controller for generator excitation over the period of 25 seconds.

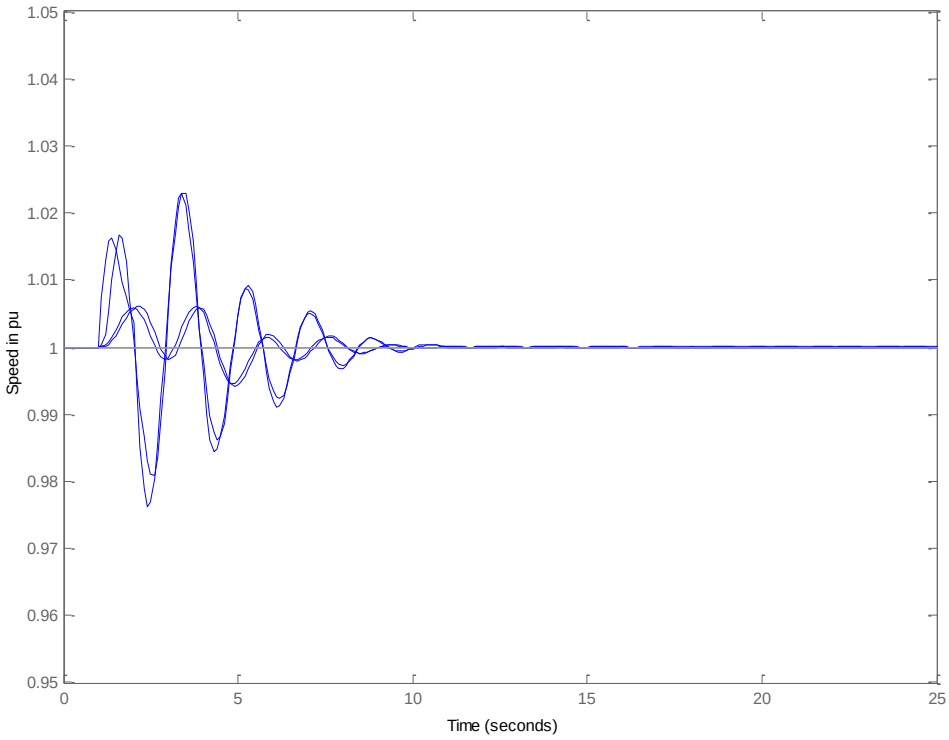

Fig. 4.6 Speeds of all generators with both PSS and MPC wide-area damping controller

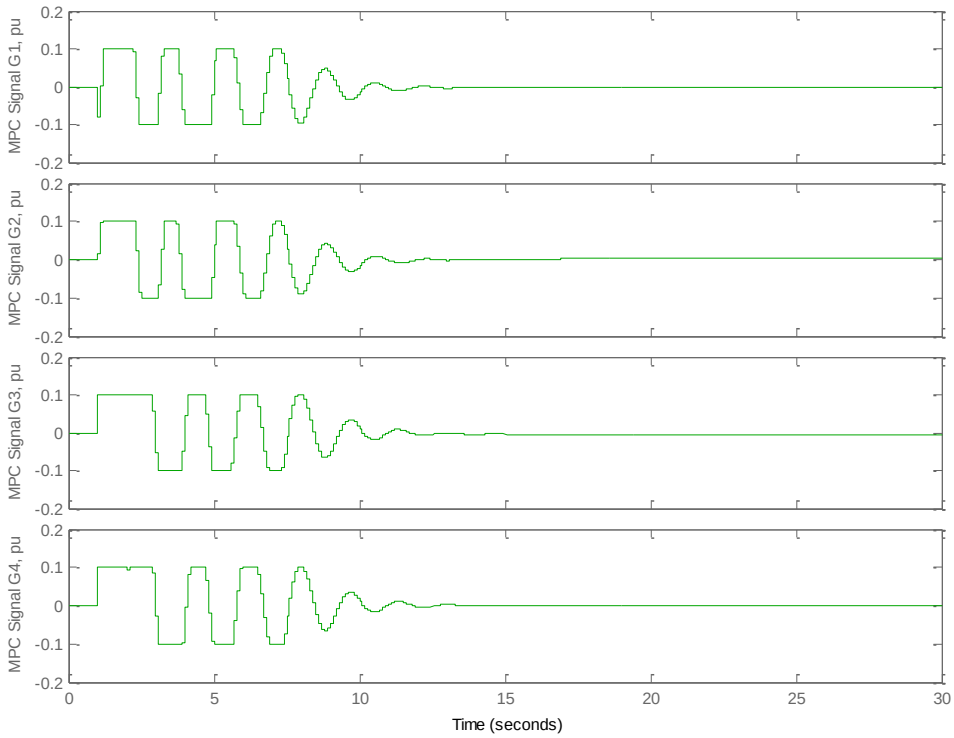

Fig. 4.7 MPC wide-area control signals to each generator

It can be observed from the above figure that all MPC wide-area signals go back to zero after the oscillations were damp out.

4.3 IEEE 16-Generator 68-Bus Test System

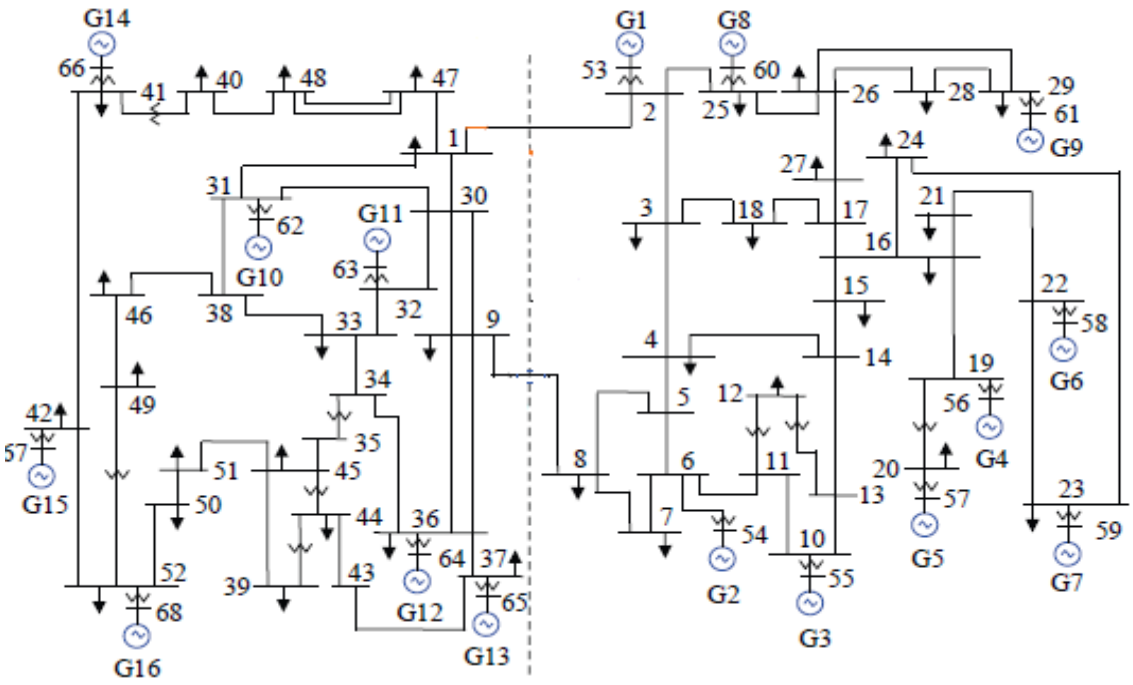

Fig. 4.8 IEEE 16-Generator 68-Bus Test System [2]

4.3.1 Test System Description

IEEE 16-machines, 5-Area test system is shown in Fig. 4.8. This is a reduced equivalent of the interconnected New England Test System (NETS) and New York Power System (NYPS). There are five geographical regions out of which NETS and NYPS are represented by a group of generators whereas, import from each of the three other neighboring areas, namely area 3, 4, and 5, are approximated by equivalent generator models.

Generator G1 to G9 are the equivalent representation of the NETS generation whilst machines G10 to G13 represent the generation of the NYPS. Generators G14 to G16 are dynamic equivalents of the three neighboring areas connected to the NYPS. In steady-state, the tie-line power exchange between NETS and NYPS is 700MW in total.

All the generators use subtransient model, with identical simple exciters, thermal turbines and governors modeled on all generators. Local power system stabilizers are installed on G1 to G12 with rotor speeds as input. The active loads are 50% constant impedance while reactive loads are all constant impedance.

4.3.2 Full-order Model and Small Signal Analysis

With the detail model, generators 1 to 12 have 15 states while generators 13 to 16 have 9 states bringing the total number of generator states to 216. There are 33 states for active load modulation and another 33 for reactive load modulation which bring the total number of states for the whole test system to 282.

The non linear model is linearized around an operating point by *svm_mgen*. The MATLAB script file, *svm_mgen*, is a Power System Toolbox (PST) driver which calls the models of the PST to

- Select a data file
- Perform a load flow
- Form a linearized model by perturbing each state in turn
- Do a modal analysis of the system

After running *svm_mgen*, the small signal analysis shows that this system has several local and inter-area modes with damping ratio less than 5 per cent. Fig. 4.9 shows the plot of frequency against damping ratio of the system's modes.

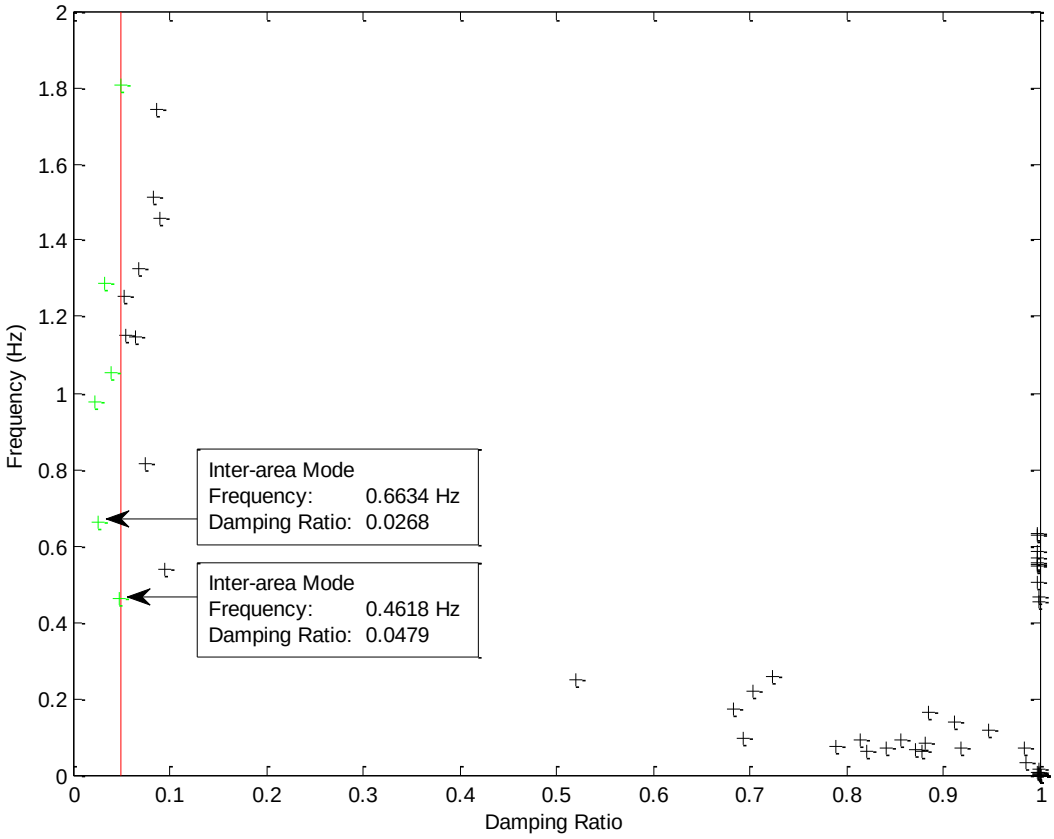

Fig. 4.9 Calculated Modes of IEEE 16-Generator 5-Area Test System

Table 4.2 Classification of Electromechanical Oscillation for modes shown in Fig. 4.9

Mode Index	Mode Type	Frequency (Hz)	Damping Ratio
1	Inter-area	0.4618	0.0479
2	Inter-area	0.6634	0.0268
3	Local	0.9759	0.0223
4	Local	1.0523	0.0398
5	Local	1.2868	0.0321
6	Local	1.8079	0.0490

The classification of these modes is given in Table 4.2 above. Modes 1 and 2 are inter-area modes while mode 3, 4 and 5 are local modes. Note that local modes appear even though PSS were installed; this is a typical behavior of very large and complicated power systems. Their effect is not of concern, however, in spite of their low damping ratios as they will die-out quickly due to their relatively large frequencies. It is therefore not necessary to provide supplementary damping to these modes.

Mode shape and eigenvectors

The eigenvector associated with a mode indicates the relative change in the states which would be observed when the mode of oscillation is excited. Fig. 4.10 shows the compass plot of rotor angle terms of inter-area mode eigenvector. It enables us to confirm this mode (0.4618 Hz) is an inter-area mode, since aggregate generators in area 3, 4 and 5 are oscillating against generators in area 1 and 2.

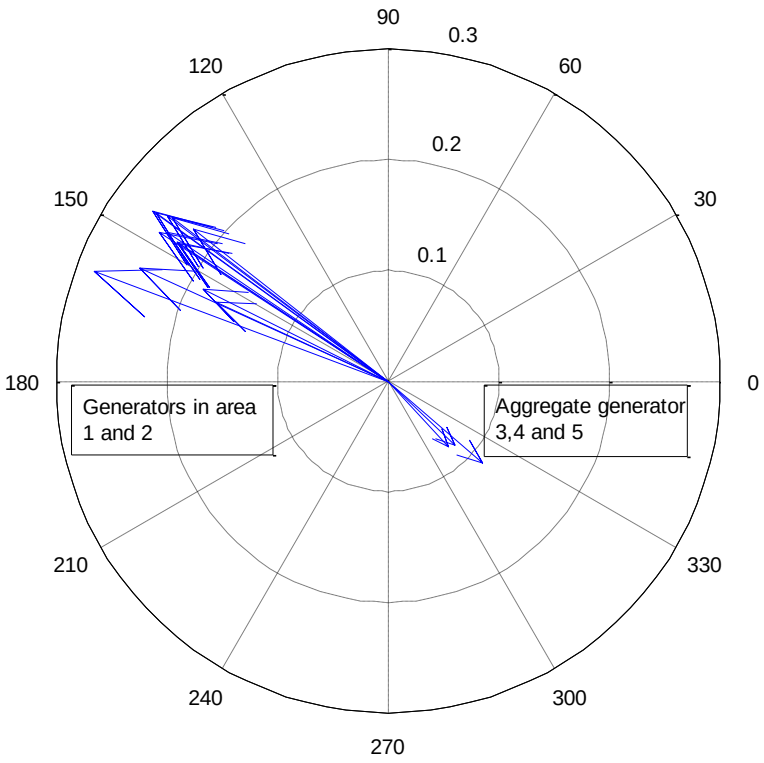

Fig. 4.10 Compass Plot of Rotor Angle Terms of Inter-area (0.4618 Hz) Mode Eigenvector

4.2.3 Control objectives and constraints

Small signal analysis shows that this system has 2 lightly damped inter-area modes $-0.1392 \pm j2.9016$ and $-0.1118 \pm j4.1638$ with frequencies of 0.4618 Hz and 0.6634 Hz respectively. The primary control objective of this MPC damping controller is aimed at achieving an acceptable damping of these modes.

Constraints are imposed on the control signal u as:

$$-0.1 \leq u \leq 0.1$$

These constraints were imposed on the MPC wide-area signal to avoid an excessive interference between wide-area damping control and the local control provided by PSS.

4.2.4 Controller Synthesis

The MPC state vector x contains 6×16 generator states, 3×12 exciter states, 3×12 PSS states, 3×16 turbine governor states. Also, there are 33 states for active modulation and another 33 for reactive modulation. The total number of states is 282. Output y is the vector of angular speeds, with reference y_{ref}, which is the unit vector of dimension 16. Input vector u consists of 12 supplementary inputs to the excitation system of each generator G1 to G12.

- Controller Tuning

The following parameters need to be specified when designing MPC controller: Prediction Horizon (N_P), Control Horizon (N_C), Weights ($W_y, W_u, W_{\Delta u}$), and Sampling Period, Δt.

Although the values of these parameters are normally guided by heuristics, there are some general guidelines for their selection to ensure satisfactory closed-loop performance and well-posed optimization [30].

Prediction and Control Horizons

For the proposed MPC controller, desired response was achieved by setting:

Prediction horizon, $N_P = 75$

Control Horizon, $N_C = 10$

Weights

The following weights were found to provide satisfactory performance.

Weights on manipulated variables, W_u = 0.01

Weights on manipulated variable rates, $W_{\Delta u}$ = 0.1

Weights on the output signal of G1 to G12, W_y = 10

Weights on the output signal of G13 to G16, W_y = 0

The weights of output signals to generator 13 to 16 are set to zero because MPC signals were not sent to these generators since they are a group of aggregated generators.

Sampling Interval

Sampling interval, Δt = 0.1 seconds

4.2.5 Simulation and Results

In order to fully test the effectiveness and robustness of the proposed MPC wide-area damping controller, the following two disturbances are considered:

- Simulation scenario 1: An impulse signal at the input mechanical torque of generator 12

In this case scenario, the disturbance used is an impulse signal applied to the input mechanical torque of generator 12 (see Fig. 4.8) in order to excite the inter-area oscillations. The time response of linear closed-loop system is used to verify the performance of the controller. Note that the disturbance is applied at $t = 1\,second$, because it is a good practice to run a simulation for a short time before applying a disturbance as this checks that the system has a satisfactory, stable initial conditions. Fig. 4.11 shows the simulated responses for this command over a period of 25s. When no MPC wide-area controller is used, sustained, slowly damped oscillations were observed.

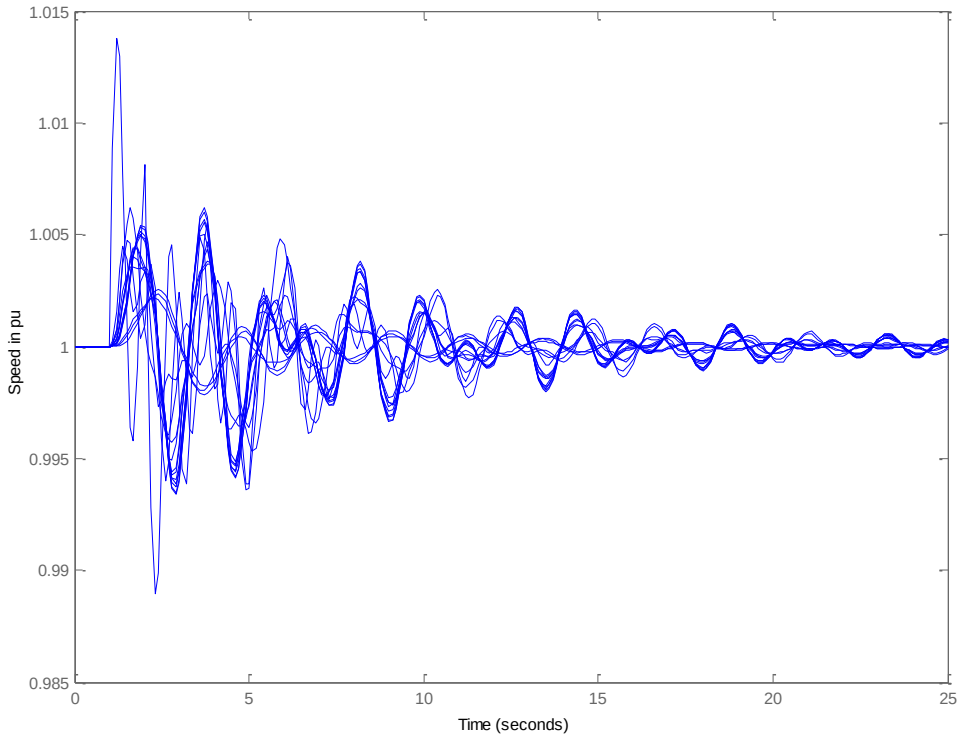

Fig. 4.11 Speeds of all Generators with PSS on G1 to G12 (No MPC Controller)

Next the MPC wide-area controller is introduced; Fig. 4.12 shows a response over a period of 25s. Compared with the system response without MPC controller (Fig. 4.11), it is observed that MPC wide-area damping controller damps the inter-area oscillations efficiently (Settling time is reduced to approximately 8 seconds). Fig. 4.13 shows the control signals computed by MPC controller to the excitation system of generator 1,2,11 and 12 over the period of 25 seconds.

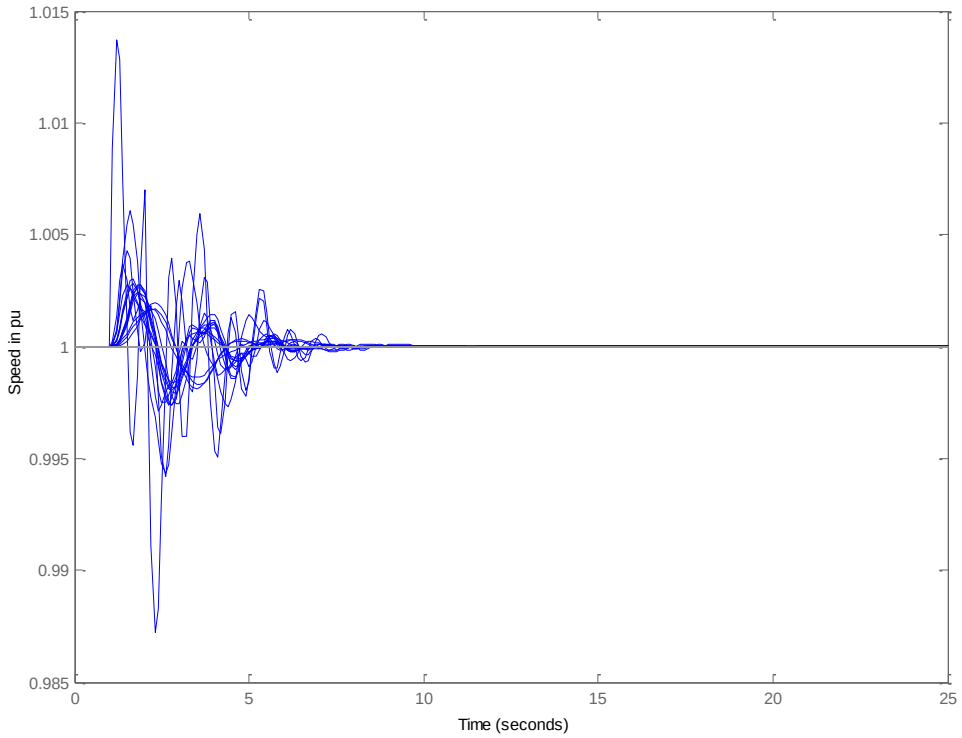

Fig. 4.12 Speeds of all Generators with both PSS and MPC wide-area damping controllers

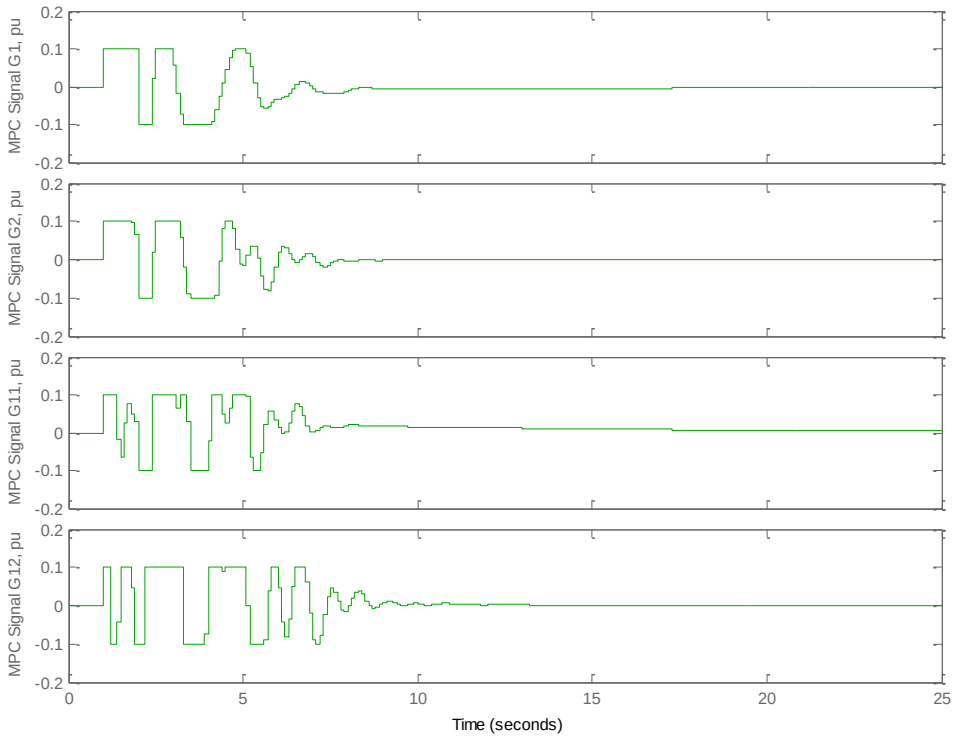

Fig. 4.13 MPC Wide-area Signals to G1, G2, G11 and G12

Fig. 4.14 shows the action of the proposed MPC wide-area controller. It is the speed deviation of generator 1 with and without MPC wide-area damping controller.

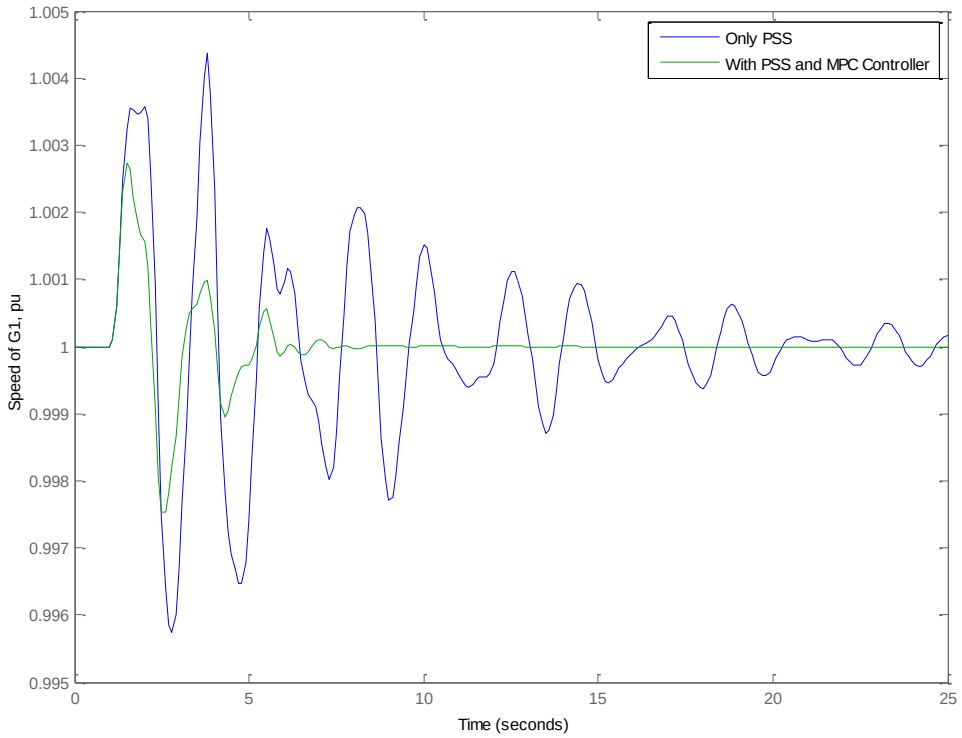

Fig. 4.14 Speed of Generator 1 (with and without MPC wide-area damping controller)

- Simulation scenario 2: An impulse signal is applied to exciter reference voltage of generator 12

In this case scenario, the disturbance used is an impulse signal applied to the exciter reference voltage of generator 12 (Fig. 4.8) in order to excite the inter-area oscillations. The time response of linear closed-loop system is used to verify the performance of the controller.

Fig. 4.15 shows the simulated response for this command over a period of 25s. When no MPC wide-area controller is used, a sustained, slowly damped oscillations is observed.

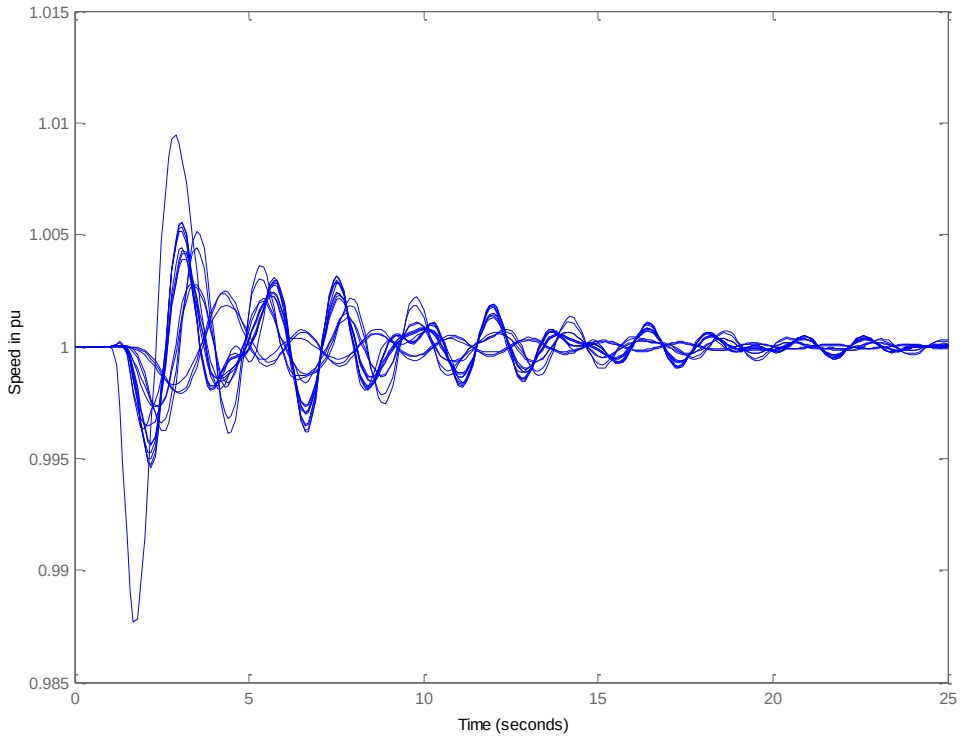

Fig. 4.15 Speeds of all generators with PSS on G1 to G12 (No MPC controller)

Next, the same MPC wide-area controller of case scenario 1 is introduced in order to investigate the robustness of the design controller; Fig. 4.16 shows a response over a period of 25s.

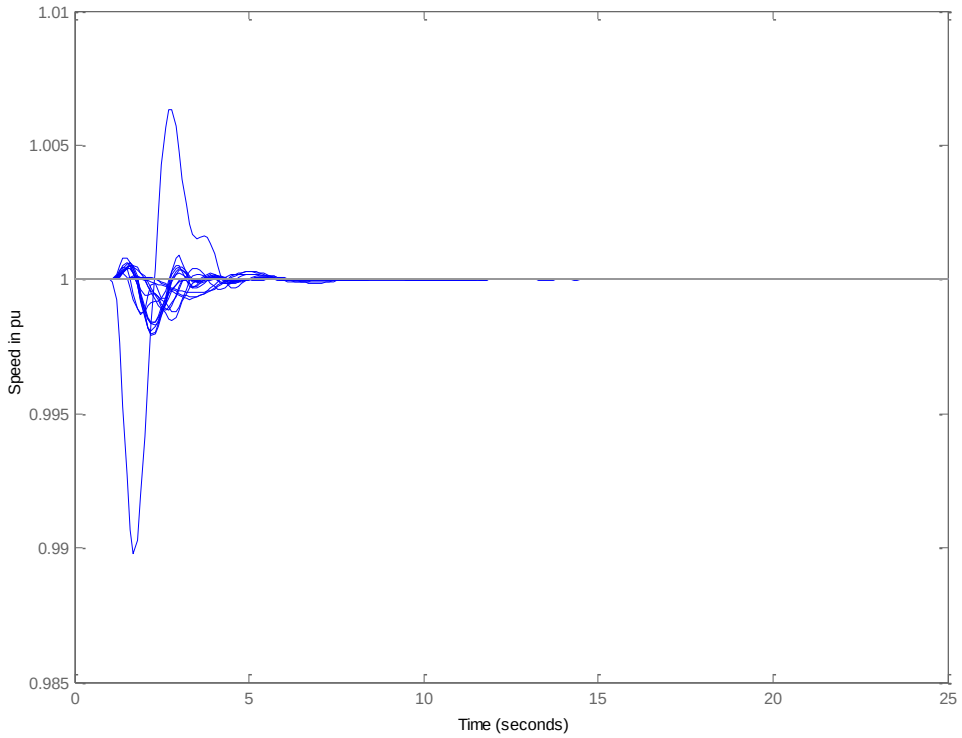

Fig. 4.16 Speeds of all Generators with both PSS and MPC wide-area damping controller

Compared with the system response without MPC controller (Figure 4.15), it is observed that MPC wide-area damping controller damps the inter-area oscillations effectively (Settling time is reduced to approximately 5 seconds). This proves that the designed controller is robust and can damp oscillations generated by variety of disturbances.

CHAPTER 5
CONCLUSION AND FUTURE WORK

5.1 Conclusion

This thesis develops a systematic procedure of designing Wide-Area Damping Controller (WADC) using Model Predictive Control (MPC) technique to damp inter-area oscillations in power systems.

MPC presents a dramatic advancement in the theory of modern automatic control. It was originally studied and applied in the process industry, where it has been in use for decades. At a control instant, the MPC algorithm optimizes a performance index with respect to some future control sequence, using predictions of the output signal based on the system model, while satisfying constraints on inputs and output/states.

The proposed technique is based on a linearized discrete-time state space model of a power system. The MPC controller computes the optimal input sequence over a chosen time horizon by solving a quadratic programming problem and sends these signals to the excitation system of a remote generator where it will supplement the local damping controllers. Power System Stabilizers were used as local damping controllers for in this thesis.

To study and control power system oscillations, a complete power system, including synchronous generator, excitation system, governor and power system stabilizer are required to be modeled. The proposed MPC scheme is outline, with detail state space formulation, prediction and cost function optimization

The effectiveness and robustness of the proposed Model Predictive Controller for wide-area damping control scheme have been verified by two study systems. The first test system is the IEEE 4-Generator 2-Area test system. The second one is the IEEE 16-Generator 68-Bus test system.

Simulation results of these test systems reveal that the proposed MPC wide-area damping controller damps inter-area oscillations effectively under varying operating conditions and different disturbances.

5.2 Future Work

This thesis propose an MPC wide-area damping scheme that computes all control signals in a centralize way. In order to comply with practical constraints of very large scale interconnected power systems, a multi-layer and distributed MPC scheme will be more suitable. In this scheme, fast updates of control will be carried out in the lower layer based on detail models of smaller sub-areas, while slower updates of controls would be used to coordinate these at the higher layers based on aggregation of the models of the lower layers.

The approached employ in this thesis is to design MPC wide-area controller that provides control actions through generator excitation systems supplemental to the action of local PSSs. The controller design effort can be extended to include FACTS devices because they can change the power flow on tie-lines directly and thus damp power oscillations more efficiently.

The effect of time delay is not considered. In practice, delay is inevitable and an important consideration in wide-area damping control. Depending on the distance of the measurement sites and transmission protocol, different amount of delays for each signal need to be considered during the design. This would be an important area for further research.

BIBLIOGRAPHY

1. M. Klein, G. J. Rogers and P. Kundur, "A Fundamental Study of Inter-area Oscillations in Power Systems," IEEE Transactions on Power Systems, Vol. 6, No. 3, pp. 914-921, August 1991

2. G. Rogers, Power System Oscillations. Norwell, Massachusetts, USA: Kluwer Academic Publishers, 2000

3. P. Kundur, Power System Stability and Control. New York: McGraw-Hill, 1994

4. E. V. Larsen and J. H. Chow, SVC Control Design Concepts for System Dynamic Performance, in IEEE Special Publications: Application of Static VAR Systems for System Dynamic Performance, pp. 36 – 53, 1987

5. K. Innocent and L. Gerin-Lajoie, "State-Space System Identification – Toward MIMO Models for Modal Analysis and Optimization of Bulk Power System", IEEE Trans. on Power Systems, Vol. 15, No.1, Feb, 2000

6. C. Taylor, D. Erickson, E. Martin, V. Venkatasubramanian, "WACS – Wide-area Stability and Voltage Control System: R&D and Online Demonstration", Proceedings of the IEEE, Vol. 93, No. 5, MAY 2005

7. N. Martins, A. Barbosa, J. Ferraz, M.G. Santos, "Retuning Stabilizers for the North-South Brazilian Interconnection", IEEE PES Summer Meeting, 18-22 July, 1999, Vol. 1, pp. 58-67

8. H. Breulman, E. Grebe, M. Losing, W. Winter, R. Witzman, P. Dupuis, "Analysis and Damping of Inter-area Oscillations in the UCTE/CENTREL Power Systems", CIGRE 2000 in Paris, pp. 38-113

9. U.S. – Canada Power System Outage Task Force: Final Report on the August 14, 2003 Blackout in the United States and Canada (on line): http://www.pserc.wisc.edu/BlackoutFinal-Web.pdf

10. J. Ma, T. Wang, Z. Wang, and J. Wu, "Design of Global Power Systems Stabilizer to Damp Inter-area Oscillations Based on Wide-Area Collocated Control Techique,"

11. M. Klein, G. J. Rogers, S. Moorty, P. Kundur, "Analytical Investigation of Factors Influencing Power System Stabilizers Performance," IEEE Trans. PWRS, Vol. EC-7, Sept 1992, pp 382-388

12. A. Sallam, J. McCalley, and A. Fouad, "Damping Controller Design for Power System Oscillations using global signals," IEEE Trans. Power Syst., vol. 11, no. 2, pp. 767-773, May 1996

13. W.A. Mittelstadt, PE. Krause, P.N. Overholt, J.F. Hauer, R.E. Wilson, D.T. Rizy, "The DOE Wide-area Measurement System (WAMS) Project - Demonstration of Dynamic Information Technology for Future Power System," Fault and Disturbance Analysis & Precise Measurements in Power Systems, Arlington, VA, Nov, 1995

14. A. G. Phadke, "Synchronized Phasor Measurements – a historical overview", In Proc. IEEE/PES Transmission and Distribution Conference and Exhibition, pp. 416-479, 2002

15. I. Kamwa, J. Beland, G. Trudel, R. Grondin, C. Lafond, and D. McNabb, "Wide-Area Monitoring and Control at Hydro-Québec: Past, Present and Future," in Proc. IEEE PES Summer Meeting, pp.1-12, 18-22 June 2006

16. I. Kamwa, A. Heniche, G. Trudel, M. Dobrescu, R. Grondin and D. Lefebvre, "Assessing the technical value of FACTS-based wide-area damping control loops," IEEE/PES General Meeting, Vol. 2, pp.1734 –1743, 12-16 June, 2005

17. K. Tomsovic, D.E. Bakken, V. Venkatasubramanian, A. Bose, "Designing the Next Generation of Real-time Control, Communication, and Computations for Large Power Systems," Proc. IEEE Vol: 93, Issue: 5, pp. 965-979, May 2005

18. I. Kamwa, R. Grondin, and Y. Hebert, "Wide-area Measurement Based Stabilizing Control of Large Power Systems – A decentralized/ hierarchical approach," IEEE Trans. Power Systems, Vol. 16, No. 1, pp. 136 – 153, Feb. 2001

19. Y. Zhang and A. Bose, "Design of Wide-area Damping Controllers for Inter-area Oscillations," IEEE Trans. Power Systems. Vol. 23, No. 3, pp. 1136-1143, August 2008

20. Ni H., Heydt G.T. and Mili L., "Power System Stability Agents Using Robust Wide-Area Control", IEEE Control System Magazine, Vol. 20, pp.82-90, Aug. 2000

21. P. S. Dolan, J. S. Smith and W. A. Mittelstadt, "A Study of TCSC Optimal Damping Control Parameters for Different Operating Conditions", IEEE Transactions on Power Systems, Vol. 10, No. 4, pp. 1972 – 1978, November, 1995

22. C. Li, X. Chen and Z. Ma, "Design of a Wide-area PSS for Damping Inter-area low-frequency Oscillations", Proc. Of the 5th IEEE Conference on Industrial Electronics and Applications, Georgia, USA, pp. 808-813, 2010

23. J. M. Maciejowski, “Predictive Control with Constraints”, Harlow, England: Prentice Hall, 2002

24. E. F. Camacho and C. Bordons, “Model Predictive Control”, Second Edition, Sringer – Verlag, London, 2007

25. J. A. Rossiter, “Model-Based Predictive Control: A practical Approach”, CRC Press, 2004

26. L. Wang, “Model Predictive Control System Design and Implementation Using MATLAB”, Sringer – Verlag, London, 2009

27. Richalet, J. A., A. Rault, J. L. Papon (1978), “Model Predictive Heuristic Control: application to an industrial process”, Automatica, 14, 413-428

28. Cutler, C. R. and B. L. Ramaker, “Dynamic Matrix Control – a computer control algorithm. AIChE National Mgt, Houston, Texas (1979)

29. Prett, D. M. and R. D. Gillette, “Optimization and Constrained Multivariable Control of a Catalytic Cracking Unit. AIChE National Mgt, Houston, Texas (1979)

30. Ogunnaike B. A and Ray W. H, “Process Dynamics, Modeling, and Control”, Oxford University Press, New York, 1994

31. Zadeh, L. A. and Whalen, “On Optimal Control and Linear Programming”, IRE Trans. Automatic Control, 7(4), 45

32. A. I., Propoi,. “Use of LP Method for Synthesizing Sampled-data Automatic Systems. Automn. Remote Control, 24:837, 1963

33. Gutman, P. O. “Controllers for Bilinear and Constrained Linear Systems”, Ph.D. Thesis, Lund Institute of Technology

34. Chang, T. S. and D. E. Seborg, “A Linear Programming Approach to Multivariable Feedback Control with inequality constraints. Int. Journal on Control, 37, 583 – 597

35. Garcia, C.E. and Morari, M. “Internal Model Control. 1. A Unifying Review and Some New Results”, Ind.Eng. Chem. Process. Des. Dev, 21:308 – 323, 1982

36. C. Garcia, D. Prett and M. Morari, “Model Predictive Control: Theory and Practice – a survey. Automatica, 25(3) pp. 335-348, 1989

37. Morari, A. and Zafiriou, A. “Robust Process Control”, Prentice-Hall, Englewood Cliffs, New Jersey, 1989

38. R. Keyser, A. Velde and F. Dumortier, “A Comparative Study of Self-adaptive Long-range Predictive Control Methods” Automatica, Vol. 24, (Issue 2), pp.149-163, 1988

39. Scattonini and Bittanti, “On the Choice of the Horizon in Long-range Predictive Control – Some Simple Criteria”, Automatica, Vol. 26, (Issue 5), pp. 915-917, 1990

40. Clarke and Scattolini, “Constrained Receding-Horizon Predictive Control”, IEEE Proceedings-D, Vol. 138 (Issue 4), July 1991

41. Bemporad, A. and Morari, M. “Robust Model Predictive Control: A Survey”, Automatic Control Laboratory, Swiss Federal Institute of Technology (ETH), 1999

42. S. Qin and T. Badgwell, “A survey of Industrial Model Predictive Control Technology”, Control Engineering Practice, Vol. 11, 2003, pp. 733 – 764

43. Mayne D. Q. and Michalska H., “Receding Horizon Control of Nonlinear Systems”, IEEE Trans. on Autom. Control, 35, pp. 814-824, 1990

44. Balchen J. G., Ljungquist D. and Strand S., “State-space Predictive Control”, Chemical Engineering Science, 47, pp. 787-807, 1992

45. Becerra V. M., Roberts P.D and Griffiths G.W., “Novel Developments in Process Optimization Using Predictive Control”, J. Proc. Cont., 8, pp. 117-138, 1998

46. M. Abu-Ayyad, R. Dubay, “Real-time comparison of a number of predictive controllers”, ISA Transaction, Vol. 46, 2007, pp. 411-418

47. Lee, J. H. “Model Predictive Control: Review of the Three Decades of Development”, Int. J. Control Automat. Sys., vol. 9, no. 3, pp. 415-424, 2011

48. Morari, M. and Lee, J. H. “Model Predictive Control: Past, Present and Future”, Comput. Chem. Eng., vol. 23, nos. 4-5, pp. 667-682, May 1999

49. Rodriguez J., Kazmierkowski M.P., Espinoza J.R., Zanchetta P.et al., “State of the Art of Finite Control Set Model Predictive Control in Power Electronics”, IEEE Transaction on Industrial Informatics, Vol. 9, Issue 2, pp. 1003-1016

50. Vazquez S., Leon J.I., Franquelo L.G., Rodriguez Y., et al., “Model Predictive Control: A Review of Its Applications in Power Electronics”, IEEE Industrial Electronics Magazine, Vol. 8, Issue 1, pp. 16-31, 2014

51. Samir K., Patricio C., Rene V., et al "Model Predictive Control – A Simple and Powerful Method to Control Power Converters", IEEE Transactions on Industrial Electronics, Vol. 56, NO. 6, June 2009

52. Xiangjie L., Xiaobing K., Xizhi D., Power System Model Predictive Load Frequency Control", American Control Conference, pp. 6602-6607, 2012

53. Lianfang K., Lei X., "A New Model Predictive Control Scheme-Based Load-Frequency Control", IEEE International Conference on Control and Automation, pp. 2514-2518, 2007

54. Jin L., Kumar R., Elia N., "Application of Model Predictive Control in Voltage Stabilization", American Control Conference, pp. 5916-5921, 2007

55. Moradzadeh M., Bhojwani L., Boel R., "Coordinated Voltage Control via Distributed Model Predictive Control", Chinese Control and Decision Conference (CCDC), pp. 1612-1618, 2011

56. Nguyen T.T., Wagh S.R., "Model Predictive Control of FACTS Devices for Power System Transient Stability", Transmission and Distribution Conference and Exposition: Asia and Pacific, pp. 1-4, 2009

57. Phulpin Y., Hazra J., Ernst D., "Model Predictive Control of HVDC Power Flow to Improve Transient Stability in Power Systems", IEEE International Conference on Smart Grid Communications (SmartGridComm), pp. 593-598

58. Licheng Jin, Kumar R., Elia N., "Model Predictive Control-Based Real-Time Power System Protection Schemes", IEEE Transactions on Power Systems, Vol. 25, Issue 2, pp. 988-998, May 2010

59. Larsson M., Karlsson D., "Coordinated System Protection Scheme Against Voltage Collapse Using Heuristic Search and Predictive Control", IEEE Transaction on Power Systems, Vol. 18, Issue 3, pp. 1001-1006, 2003

60. Halvgaard R., Poulsen N.K., Madsen, H., Jorgensen J.B., "Economic Model Predictive Control for Building Climate Control in a Smart Grid", IEEE PES Innovative Smart Grid Technologies (ISGT), pp. 1-6, 2012

61. Rahnama S., Stoustrup J., Rasmussen, H., "Model Predictive Control for Integration of Industrial Consumers to the Smart Grid Under a Direct Control Policy", IEEE International Conference on Control Applications (CCA), pp. 515-520, 2013

62. D. Wang, M. Glavic and L. Wehenkel, "A New MPC Scheme for Damping Wide-area Electromechanical Oscillations in Power Systems", Proceedings of the 2011 IEEE PES PowerTech, Trondheim, Norway, June, 2001

63. D. Wang, M. Glavic and L. Wehenkel, "Distributed MPC of Wide-area Electromechanical Oscillations of Large-scale Power Systems", Proceedings of the 2011 IEEE PES PowerTech, Trondheim, Norway, June, 2001

64. L. Wang, H. Cheung, A. Hamlyn and R. Cheung, "Model Predictive Adaptive Control of Inter-area Oscillations in Multi-generator Power System", Proceedings of the IEEE PES General Meeting, Calgary, Canada, pp. 1-7, 2009

65. K. Luo, Y. Liu and H. Ye, "Wide-area Damping Controller Based on Model Prediction and Sliding Mode Control", Proceedings of the 8th World Congress on Intelligent Control and Automation

66. G. Rogers and J. Chow, "Power System Toolbox, Version 3.0", Ontario K0K 1S0, Canada, 1991 – 2008

67. Peter W. Sauer, M. A. Pai, “Power System Dynamics and Stability”, Prentice Hall, 1997

68. Byerly, R. T., and Kimbark, E. W., Ed., “Stability of Large Electric Power Systems”, New York: IEEE Press, 1954

69. IEEE Committee Report, “Excitation System Models for Power System Stability Studies”, IEEE Transaction of Power Apparatus and Systems, vol. PAS-100, pp. 494-509, 1981

70. B. Miroslav, B. Mirosevic, D. Novosel, “A Novel Method for Voltage Instability Protection”, Proceeding of the 35th Hawaii International Conference on System Science, 2002

71. A. M. Lyapunov, “Stability of Motion”, Academic Press, New York, NY, 1966

72. IEEE/ PES Power System Stability Subcommittee, “Voltage Stability Assessment: Concepts, Practices and Tools. IEEE Special Publication, Technical Report SP101PSS, August 2002

73. Allgower, F., and A. Zheng, “Nonlinear Model Predictive Control”, Springer-Verlag, 2000.

74. M. Morari, N. L. Ricker, A. Bemporad, “Model Predictive Control Toolbox™ User’s Guide”, R2013a, The MathWorks, Inc. 2005-2013

75. J.H. Chow and K.W. Cheung, “A toolbox for power system dynamics and control engineering education and research”, IEEE Transactions on Power Systems, vol.7, no.4, pp.1559-1564, Nov 1992.

APPENDIX

Appendix A

IEEE 4-Generator 2-Area Test System Parameters

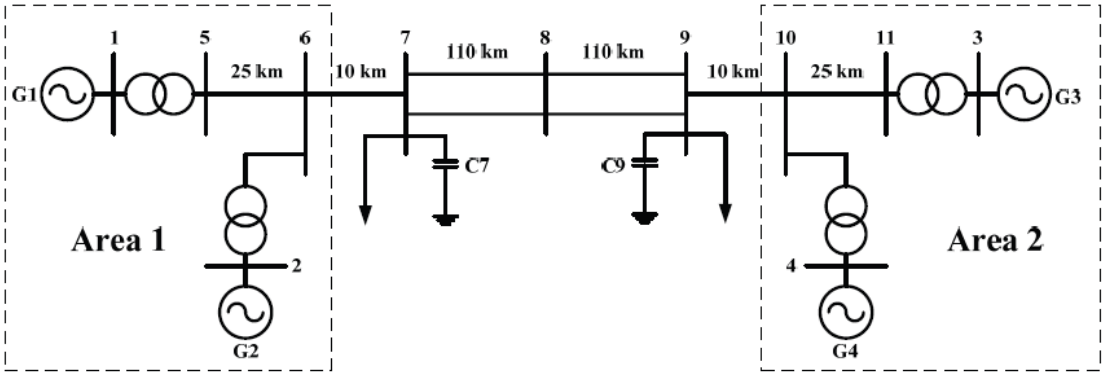

Figure A.1 Single line diagram of IEEE 4-Generator 2-area test system

The single line diagram of IEEE 4-generator 2-area test system is shown in the above Figure A.1. This system consists of two similar areas connected by weak tie. Each area consist of two coupled units, each having a rating of 900 MVA and 20 kV. The generator parameters in per unit on the rated MVA and kV base are as follows:

$X_d = 1.8$ $X_q = 0.03$ $X_l = 0.2$ $X_d^{'} = 0.3$ $X_q^{'} = 0.55$

$X_d^{''} = 0.0025$ $X_q^{''} = 0.25$ $R_a = 0$ $T_{d0}^{'} = 8.0\ s$ $T_{q0}^{'} = 0.4\ s$

$T_{d0}^{''} = 0.03\ s$ $T_{q0}^{''} = 0.05\ s$ $A_{sat} = 0.015$ $B_{sat} = 9.6$ $\psi_{T1} = 0.9$

$H = 6.5$ (for G1 and G2) $H = 6.175$ (for G3 and G4) $K_D = 0$

Each step-up transformer has an impedance of 0+j0.15 per unit on 900 MVA and 20/30 kV base, and has an off-nominal ratio of 1.0.

The transmission system nominal voltage is 230 kV. The line lengths are identified in Fig. A.1. The parameters of the lines in per unit on 100 MVA, 230 kV base are:

$r = 0.0001$ pu/km $\quad x_L = 0.001$ pu/km $\quad b_C = 0.00175$ pu/km

The system is operating with area 1 exporting 400 MW to area 2, and the generating units are loaded as follows:

G1: $P = 700\ MW,\quad Q = 185 MVAr,\quad E_t = 1.03\angle 20.20^o$

G2: $P = 700\ MW,\quad Q = 235\ MVAr,\quad E_t = 1.01\angle 10.5^o$

G3: $P = 719\ MW,\quad Q = 176\ MVAr,\quad E_t = 1.03\angle -6.8^o$

G4: $P = 700\ MW,\quad Q = 202\ MVAr,\quad E_t = 1.01\angle -17.0^o$

The loads and reactive power supplied (Q_C) by the shunt capacitors at buses 7 and 9 areas are as follows:

Bus 7: $P_L = 976\ MW, Q_L = 100 MVAr, Q_C = 200\ MVAr$

Bus 9: $P_L = 1767\ MW, Q_L = 100 MVAr, Q_C = 350\ MVAr$

Self-excited dc exciter

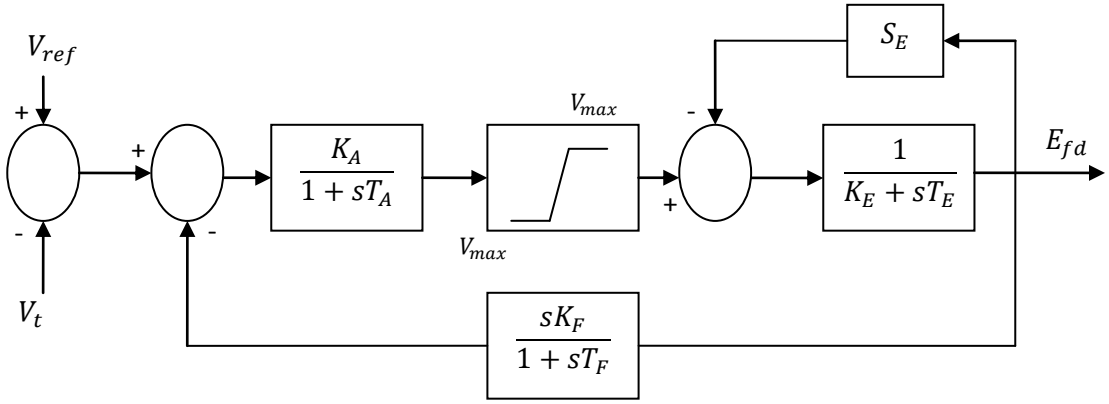

Figure A.2 IEEE type 1 self-excited dc excitation system model

In this system, uniform IEEE type 1 self-excited dc excitation system is used. Its model is shown in Figure A.2 and the parameters are as follow:

$K_A = 20.0$ $T_A = 0.05$ $T_E = 0.785$ $K_E = 1.0$ $K_F = 0.125$ $T_B = 0$

$T_F = 1.0$ $A_{ex} = 0.0056$ $B_{ex} = 1.075$ $V_{RMIN} = 10$ $V_{RMAX} = 10$ $T_C = 0$

Power System Stabilizer

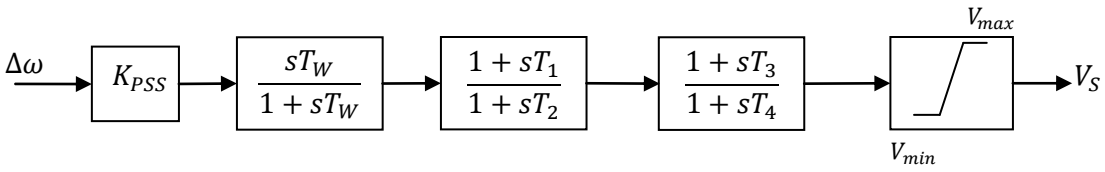

Figure A.3 Power System Stabilizer Model

$K_{STAB} = 20.0$ $T_W = 10.0$ $v_{min} = -0.05$ $v_{max} = 0.2$

$T_1 = 0.05$ $T_2 = 0.02$ $T_3 = 3$ $T_4 = 5.4$

Appendix B

IEEE 16-Generator 68 -Bus Test System Parameters

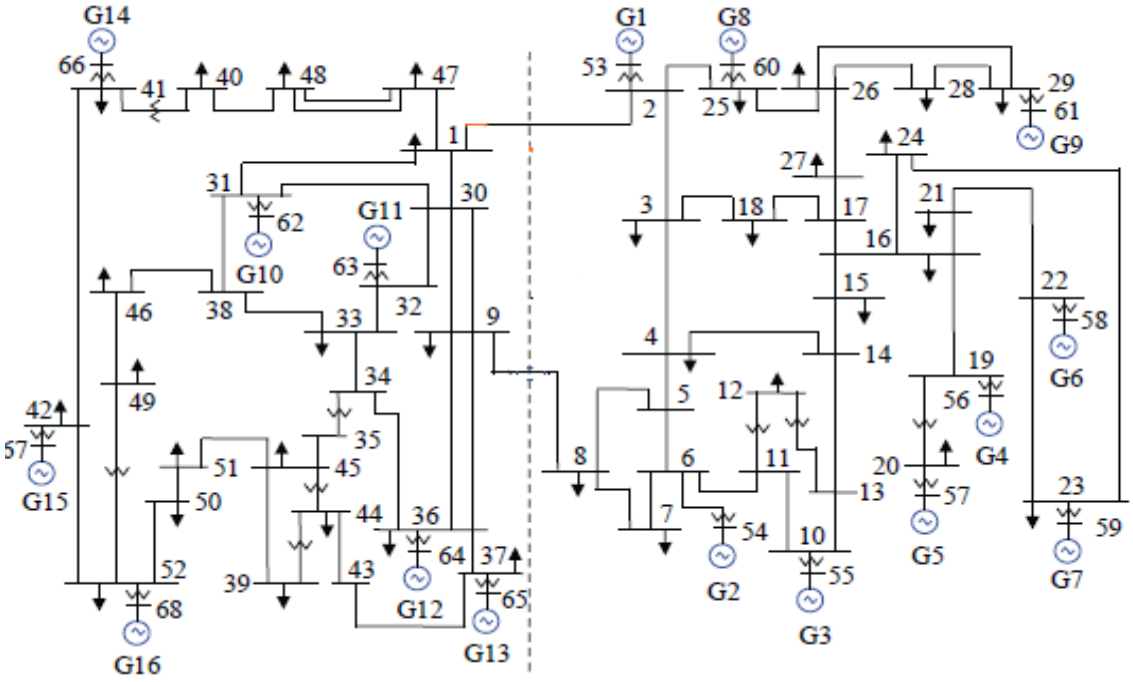

Figure B.1 Single line diagram of IEEE 16-Generator 68-Bus test system

The single line diagram of IEEE 16-Generaors 68-Bus test system is shown in Figure B.1. The parameters of the system are divided into:

- Bus Data
- Branch Data
- Generation Data
- Regulator Data

Bus Data

Table B.1 represent the bus data of IEEE 16-Generator 68-Bus system. The nomenclature for the table headings is:

Bus No. Number of the Bus

Bus Type Bus type code

(1) Slack Bus

(2) Generator Bus, PV Bus

(3) Load Bus, PQ Bus

Bus voltage Bus Voltage, in per unit

Load W Real component of the load, in per unit

Load VAR Reactive component of the Load, in per unit

Gen W Generator real power output, in per unit

Gen VAR Generator reactive power output, in per unit

Table B.1 Bus data of IEEE 16-Generator 68-bus system

Bus No.	Bus type	Bus Voltage	Load W	Load VAR	Gen W	Gen VAR
1	1	1.0	2.527	1.1856	-	-
2	1	1.0	0	0	-	-
3	1	1.0	3.22	0.02	-	-
4	1	1.0	5.0	1.84		
5	1	1.0	0	0		
6	1	1.0	0	0	-	-
7	1	1.0	2.34	0.84	-	-
8	1	1.0	5.22	1.77	-	-
9	1	1.0	1.04	1.25	-	-
10	1	1.0	0	0	-	-

11	1	1.0	0	0	-	-
12	1	1.0	0.09	0.88	-	-
13	1	1.0	0	0	-	-
14	1	1.0	0	0	-	-
15	1	1.0	3.2	1.53	-	-
16	1	1.0	3.29	0.32	-	-
17	1	1.0	0	0	-	-
18	1	1.0	1.58	0.3		
19	1	1.0	0	0		
20	1	1.0	6.8	1.03	-	-
21	1	1.0	2.74	1.15	-	-
22	1	1.0	0	0	-	-
23	1	1.0	2.48	0.85	-	-
24	1	1.0	3.09	-0.92	-	-
25	1	1.0	2.24	0.47	-	-
26	1	1.0	1.39	0.17	-	-
27	1	1.0	2.81	0.76	-	-
28	1	1.0	2.06	0.28	-	-
29	1	1.0	2.84	0.27	-	
30	1	1.0	0	0	-	
31	1	1.0	0	0	-	-
32	1	1.0	0	0		-
33	1	1.0	1.12	0		-
34	1	1.0	0	0	-	
35	1	1.0	0	0	-	
36	1	1.0	1.02	-0.1946	-	-
37	1	1.0	60	3	-	-
38	1	1.0	0	0	-	-
39	1	1.0	2.67	0.126	-	-
40	1	1.0	0.6563	0.2353	-	-

41	1	1.0	10	2.5	-	-
42	1	1.0	11.5	2.5	-	-
43	1	1.0	0	0	-	-
44	1	1.0	2.6755	0.0484	-	-
45	1	1.0	2.08	0.21	-	-
46	1	1.0	1.507	0.285	-	-
47	1	1.0	2.0312	0.3259	-	-
48	1	1.0	2.412	0.022	-	
49	1	1.0	1.64	0.29	-	
50	1	1.0	1	-1.47	-	-
51	1	1.0	3.37	-1.22	-	-
52	1	1.0	24.7	1.23	-	-
53	2	1.045	0	0	2.50	0
54	2	0.98	0	0	5.45	0
55	2	0.983	0	0	6.50	0
56	2	0.997	0	0	6.32	0
57	2	1.011	0	0	5.052	0
58	2	1.05	0	0	7.0	0
59	2	1.063	0	0	5.60	0
60	2	1.03	0	0	5.40	0
61	2	1.025	0	0	8.0	0
62	2	1.01	0	0	5.0	0
63	2	1.0	0	0	10.0	0
64	2	1.0156	0	0	13.5	0
65	3	1.011	0	0	35.91	0
66	2	1.0	0	0	17.85	0
67	2	1.0	0	0	10.0	0
68	2	1.0	0	0	40.0	0

Branch Data

Table B.2 represent the branch (transmission lines and transformers) data of IEEE 16-Generator 68-Bus system. The nomenclature for the headings is:

Number Number of the branch

From Bus Branch starting bus number

To Bus Branch ending bus number

Resistance Branch resistance, in per unit

Reactance Branch reactance, in per unit

Susceptance Branch total charging susceptance, in per unit

Branch Tap Transformer off-nominal turns ratio

Table B.2 Branch data of IEEE 16-Generator 68-bus system

Number	From Bus	To Bus	Resistance	Reactance	Susceptance	Branch Tap
1	1	2	0.0035	0.0411	0.6987	-
2	1	30	0.0008	0.0074	0.48	-
3	2	3	0.0013	0.0151	0.2572	-
4	2	25	0.007	0.0086	0.146	-
5	2	53	0	0.0181	0	1.025
6	3	4	0.0013	0.0213	0.2214	-
7	3	18	0.0011	0.0133	0.2138	-
8	4	5	0.0008	0.0128	0.1342	-
9	4	14	0.0008	0.0129	0.1382	-
10	5	6	0.0002	0.0026	0.0434	-
11	5	8	0.0008	0.0112	0.1476	-
12	6	7	0.0006	0.0092	0.1130	-
13	6	11	0.0007	0.0082	0.1389	-

14	6	54	0	0.025	0	1.07
15	7	8	0.0004	0.0046	0.078	-
16	8	9	0.0023	0.0363	0.3804	-
17	9	30	0.0019	0.0183	0.29	-
18	10	11	0.0004	0.0043	0.0729	-
19	10	13	0.0004	0.0043	0.0729	-
20	10	55	0	0.02	0	1.07
21	12	11	0.0016	0.0435	0	1.06
22	12	13	0.0016	0.0435	0	1.06
23	13	14	0.0009	0.0101	0.1723	-
24	14	15	0.0018	0.0217	0.366	-
25	15	16	0.0009	0.0094	0.171	-
26	16	17	0.0007	0.0089	0.1342	-
27	16	19	0.0016	0.0195	0.3040	-
28	16	21	0.0008	0.0135	0.2548	-
29	16	24	0.0003	0.0059	0.0680	-
30	17	18	0.0007	0.0082	0.1319	-
31	17	27	0.0013	0.0173	0.3216	-
32	19	20	0.0007	0.0138	0	1.06
33	19	56	0.0007	0.0142	0	1.07
34	20	57	0.0009	0.0180	0	1.009
35	21	22	0.0008	0.0140	0.2565	-
36	22	23	0.0006	0.0096	0.1846	-
37	22	58	0	0.0143	0	1.025
38	23	24	0.0022	0.0350	0.3610	-
39	23	59	0.0005	0.0272	0	-
40	25	26	0.0032	0.0323	0.5310	-
41	25	60	0.0006	0.0232	0	1.025
42	26	27	0.0014	0.0147	0.2396	-
43	26	28	0.0043	0.0474	0.7802	-

44	26	29	0.0057	0.0625	1.0290	-
45	28	29	0.0014	0.0151	0.2490	-
46	29	61	0.0008	0.0156	0	1.025
47	9	30	0.0019	0.0183	0.29	-
48	9	36	0.0022	0.0196	0.34	-
49	9	36	0.0022	0.0196	0.34	-
50	36	37	0.0005	0.0045	0.32	-
51	34	36	0.0033	0.0111	1.45	-
52	35	34	0.0001	0.0074	0	0.946
53	33	34	0.0011	0.0157	0.202	-
54	32	33	0.0008	0.0099	0.168	-
55	30	31	0.0013	0.0187	0.333	-
56	30	32	0.0024	0.0288	0.488	-
57	1	31	0.0016	0.0163	0.25	-
58	31	38	0.0011	0.0147	0.247	-
59	33	38	0.0036	0.0444	0.693	-
60	38	46	0.0022	0.0284	0.43	-
61	46	49	0.0018	0.0274	0.27	-
62	1	47	0.0013	0.0188	1.31	-
63	47	48	0.0025	0.0268	0.40	-
64	47	48	0.0025	0.0268	0.40	-
65	48	40	0.0020	0.022	1.28	-
66	35	45	0.0007	0.0175	1.39	-
67	37	43	0.0005	0.0276	0	-
68	43	44	0.0001	0.0011	0	-
69	44	45	0.0025	0.073	0	-
70	39	44	0	0.0411	0	-
71	39	45	0	0.0839	0	-
72	45	51	0.0004	0.0105	0	-
73	50	52	0.0012	0.0288	0.72	-

74	50	51	0.0009	0.0221	2.06	-
75	49	52	0.0076	0.1141	1.16	-
76	52	42	0.0040	0.0600	2.25	-
77	42	41	0.0040	0.0600	2.24	-
78	41	40	0.0060	0.0840	3.15	-
79	31	62	0	0.026	0	1.04
80	32	63	0	0.013	0	1.04
81	36	64	0	0.0075	0	1.04
82	37	65	0	0.0033	0	1.04
83	41	66	0	0.0015	0	1
84	42	67	0	0.0015	0	1
85	52	68	0	0.0030	0	1
86	1	27	0.032	0.032	0.41	1

Note that in Table B.2 there are several same branches which mean the double-circuit transmission lines.

Generation Data

Table B.3 represents the generation data of IEEE 16-Generator 68-bus test system. The nomenclature of the table headings is:

Unit No Number of the generators

H Inertia constant of generators, in seconds

R_a Resistance, in per unit

X_l Leakage reactance, in per unit

X_d D-axis synchronous reactance, in per unit

X_q Q-axis synchronous reactance, in per unit

X'_d D-axis transient reactance, in per unit

X'_q Q-axis open-circuit time constant, in second

T'_{do} D-axis open-circuit time constant, in second

T'_{qo} Q-axis open-circuit time constant, in second

Table B.3 Generator Data of IEEE 16-Generator 68-Bus Test System

Unit No.	H (sec)	R_a	X_l	X_d	X_q	X'_d	X'_q	T'_{do}	T'_{qo}
1	3.4	0	0.003	0.969	0.6	0.248	0.25	12.6	0.035
2	1.8	0	0.035	1.8	1.7207	0.4253	0.3661	6.56	1.5
3	4.9623	0	0.0304	1.8	1.7098	0.383	0.3607	5.7	1.5
4	4.1629	0	0.0295	1.8	1.7725	0.2992	0.2748	5.69	1.5
5	4.7667	0	0.027	1.8	1.6909	0.36	0.3273	5.4	0.44
6	4.9107	0	0.0224	1.8	1.7079	0.3543	0.3189	7.3	0.4
7	4.3267	0	0.0322	1.8	1.7817	0.299	0.2746	5.66	1.5
8	3.915	0	0.028	1.8	1.7379	0.3538	0.3103	6.7	0.41
9	4.0365	0	0.0298	1.8	1.7521	0.4872	0.4274	4.79	1.96
10	2.9106	0	0.0199	1.8	1.2249	0.4868	0.4793	9.37	1.5
11	2.0053	0	0.0103	1.8	1.7297	0.2531	0.2109	4.1	1.5
12	5.1721	0	0.022	1.8	1.6931	0.5525	0.4990	7.4	1.5
13	4.0782	0	0.003	1.8	1.7292	0.3345	0.3041	5.9	1.5
14	3	0	0.0017	1.8	1.73	0.285	0.25	4.1	1.5
15	3	0	0.0017	1.8	1.73	0.285	0.25	4.1	1.5
16	4.45	0	0.0041	1.8	1.6888	0.359	0.3034	7.8	1.5

Regulator Data

The regulators of generator used in this thesis include exciter and PSS, in the following, the parameters of these two regulators will be listed respectively.

Exciter Data

Exciter used in IEEE 16-Generator 68-Bus system is IEEE Type 1 rotating excitation system which is the same as IEEE 4-Generator 2-Area system depicted in APPENDIX A. The model of IEEE type 1 rotating excitation system is shown in Figure A.2 and Table B.4 represents the exciter data of IEEE 16-Generator 68-Bus Test System. The nomenclature of the table headings is:

Unit No.	Number of generators
K_A	Voltage regulator gain
T_A	Voltage regulator time constant, in seconds
V_{RMAX}	Maximum voltage regulator output
V_{RMIN}	Minimum voltage regulator output
K_E	Exciter constant
T_E	Exciter time constant, in second
K_F	Stabilizer gain
T_F	Stabilizer time constant, in seconds
C_1	Saturation function 1
C_2	Saturation function 2

Table B.4 Exciter data of IEEE 16-Generator 68-Bus System

Unit No	K_A	T_A	V_{RMAX}	V_{RMIN}	K_E	T_E	K_F	T_F	C_1	C_2
1	30	0.02	10	-10	1.0	0.785	0.03	1.0	0.07	0.91
2	30	0.02	10	-10	1.0	0.785	0.03	1.0	0.07	0.91
3	30	0.02	10	-10	1.0	0.785	0.03	1.0	0.07	0.91
4	30	0.02	10	-10	1.0	0.785	0.03	1.0	0.07	0.91
5	30	0.02	10	-10	1.0	0.785	0.03	1.0	0.07	0.91
6	30	0.02	10	-10	1.0	0.785	0.03	1.0	0.07	0.91
7	30	0.02	10	-10	1.0	0.785	0.03	1.0	0.07	0.91
8	30	0.02	10	-10	1.0	0.785	0.03	1.0	0.07	0.91
9	30	0.02	10	-10	1.0	0.785	0.03	1.0	0.07	0.91
10	30	0.02	10	-10	1.0	0.785	0.03	1.0	0.07	0.91
11	30	0.02	10	-10	1.0	0.785	0.03	1.0	0.07	0.91
12	30	0.02	10	-10	1.0	0.785	0.03	1.0	0.07	0.91

PSS Data

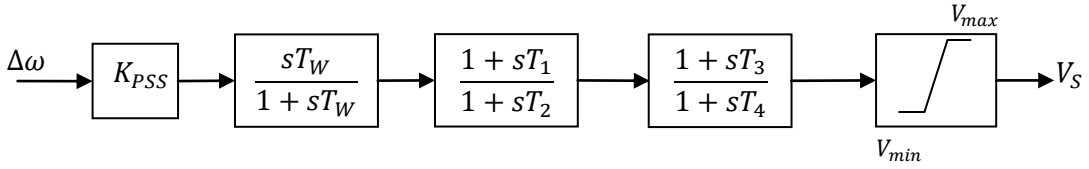

Figure B.2 IEEE PSS

Table B.4 represent the PSS data of IEEE 16-Generator 68-Bus Test System. The nomenclature of the table heading is:

Unit No Number of generators

K_{PSS} PSS gain

T_W PSS washing time, in seconds

T_1 PSS leading time constant, in seconds

T_2 PSS lag time constant, in seconds

T_3 PSS leading time constant, in seconds

T_4 PSS lag time constant, in seconds

V_{max} PSS maximum voltage output

V_{max} PSS minimum voltage output

Table B.5 PSS Data of IEEE 16-Generator 68-Bus system

Unit No	K_{PSS}	T_W	T_1	T_2	T_3	T_4	V_{max}	V_{max}
1	100	10	0.1	0.02	0.08	0.02	0.2	- 0.05
2	100	10	0.08	0.02	0.08	0.02	0.2	- 0.05
3	100	10	0.08	0.02	0.08	0.02	0.2	- 0.05
4	100	10	0.08	0.02	0.08	0.02	0.2	- 0.05
5	100	10	0.08	0.02	0.08	0.02	0.2	- 0.05
6	100	10	0.1	0.02	0.1	0.02	0.2	- 0.05
7	100	10	0.08	0.02	0.08	0.02	0.2	- 0.05
8	100	10	0.08	0.02	0.08	0.02	0.2	- 0.05
9	100	10	0.08	0.03	0.05	0.01	0.2	- 0.05
10	100	10	0.1	0.02	0.1	0.02	0.2	- 0.05
11	100	10	0.08	0.03	0.05	0.01	0.2	- 0.05
12	100	10	0.1	0.02	0.1	0.02	0.2	- 0.05

Appendix C

Power System Toolbox (PST) [34]

Introduction

The Power System Toolbox (PST) was conceived and initially developed by Dr. Kwok W. Cheung and Prof. Joe Chow from Rensselaer Polytechnic Institute in the early 1990s. From 1993 to 2009, it was marketed, and further developed, by Graham Rogers (formerly Cherry Tree Scientific Software), and is in use by utilities, consultants and universities worldwide.

PST consists of a set of coordinated MATLAB m-files which model the power system components necessary for power system power flow and stability studies. The toolbox comes with the m-files, demo examples of how the models can be used, several sets of dynamic data and a user's manuals. The original paper [75] about PST was published in the IEEE Transactions on Power Systems.

Dynamic Simulation

The Power System Toolbox provides models of machines and control systems for performing transient stability simulations of a power system, and for building state variable models for small signal analysis and damping controller design. These dynamic models are coded as MATLAB functions.
MATLAB m-files are provided which enable a user to perform transient and small signal stability analysis without adding any new models. However, since the complete code is in the form of MATLAB m-files, by following a set of rules, the user can assemble customized models and applications.

- Transient Stability Simulation

PST provides the models of machines and control systems in the form of MATLAB functions, for performing transient stability simulations, and for small signal stability

analysis and damping controller design. A solved load flow case is required to set the operating condition used to initialize dynamic device models. A fault is defined in the data specification card `sw_con'. The driving function `**s_simu**' provides a transient simulation environment which requires the data file specifying system structure, controller and faults, like stand-alone transient programs. It calculates transient response by solving a set of differential equations determined by the dynamic models and a set of algebraic equations determined by the power system network.

- Small Signal Stability

The stability of the operating point of a dynamic system to small disturbances is termed small signal stability. To test for small signal stability the system's dynamic equations are linearized about a steady state operating point to get a linear set of state equations

$$\dot{X} = Ax + Bu$$

$$y = Cx + Du$$

where A is the state matrix; B is the input matrix; C is the output matrix ; D is the feed forward matrix; x is the state vector and u is the input.

In PST, starting from the states determined from model initialization, a small perturbation is applied to each state in turn. The change in the rates of change of all the states divided by the magnitude of the perturbation gives a column of the state matrix corresponding to the disturbed state. A permutation matrix **p_mat** is used to arrange the states in a logical order. Following each rate of change of state calculation, the perturbed state is returned to its equilibrium value and the intermediate variable values are reset to their initial values. Each step in this process is similar to a single step in a simulation program. The input matrix B, the output matrix C and the feed forward matrix D can be determined in a similar manner.

A single driver, **svm_mgen**, for small signal stability is provided. It is organized similarly to the transient stability simulation driver **s_simu**. New models should be designed to work satisfactorily in either driver. Generally, if a model is satisfactory in **s_simu**, it will be satisfactory in **svm_mgen**.